BioOne COMPLETE

# Habitat of the Giant Pterosaur Quetzalcoatlus Lawson 1975 (Pterodactyloidea: Azhdarchoidea): A Paleoenvironmental Reconstruction of the Javelina Formation (Upper Cretaceous), Big Bend National Park, Texas

Author: Lehman, Thomas M.

Source: Journal of Vertebrate Paleontology, 41(sp1) : 21-45

Published By: The Society of Vertebrate Paleontology

URL: https://doi.org/10.1080/02724634.2019.1593184

BioOne Complete (complete.BioOne.org) is a full-text database of 200 subscribed and open-access titles in the biological, ecological, and environmental sciences published by nonprofit societies, associations, museums, institutions, and presses.

Your use of this PDF, the BioOne Complete website, and all posted and associated content indicates your acceptance of BioOne's Terms of Use, available at www.bioone.org/terms-of-use.

Usage of BioOne Complete content is strictly limited to personal, educational, and non - commercial use. Commercial inquiries or rights and permissions requests should be directed to the individual publisher as copyright holder.

BioOne sees sustainable scholarly publishing as an inherently collaborative enterprise connecting authors, nonprofit publishers, academic institutions, research libraries, and research funders in the common goal of maximizing access to critical research.

Downloaded From: https://bioone.org/journals/Journal-of-Vertebrate-Paleontology on 24 Apr 2024
Terms of Use: https://bioone.org/terms-of-use

Society of Vertebrate Paleontology Memoir 19
Journal of Vertebrate Paleontology
Volume 41, Supplement to Number 2:21–45
Published with license by the Society of Vertebrate Paleontology

MEMOIR ARTICLE

# HABITAT OF THE GIANT PTEROSAUR *QUETZALCOATLUS* LAWSON 1975 (PTERODACTYLOIDEA: AZHDARCHOIDEA): A PALEOENVIRONMENTAL RECONSTRUCTION OF THE JAVELINA FORMATION (UPPER CRETACEOUS), BIG BEND NATIONAL PARK, TEXAS

THOMAS M. LEHMAN
Department of Geosciences, Texas Tech University, Lubbock, Texas 79409-1053, U.S.A., tom.lehman@ttu.edu

ABSTRACT—The Maastrichtian Javelina Formation of southwestern Texas comprises a thick sequence of stream channel and floodplain deposits accumulated in a broad southeast-trending valley, several hundred kilometers inland from the Late Cretaceous shoreline. Three pterosaur species are found here. Remains of *Quetzalcoatlus lawsoni*, sp. nov., are concentrated in deposits of shallow alkaline lakes that developed in abandoned reaches of stream channels. Areas surrounding the lakes were vegetated with fan palms, and the higher floodplain supported a subtropical forest dominated by the dicot tree *Javelinoxylon* and araucariacean conifers. The shallow lakes were inhabited by a diverse invertebrate fauna of arthropods, gastropods, and bivalves, a likely food source for the slender-beaked *Quetzalcoatlus lawsoni*, sp. nov., which may have had a lifestyle similar to modern large gregarious wading birds. In contrast, remains of the giant *Q. northropi* are rare and found instead only in stream channel facies. It may have had a more solitary lifestyle and preferred riparian habitats. The warm, dry, subtropical but nonseasonal conditions of the region may represent a preferred climatic regime for azhdarchid pterosaurs generally.

Citation for this article: Lehman, T. M. 2021. Habitat of the giant pterosaur *Quetzalcoatlus* Lawson 1975 (Pterodactyloidea: Azhdarchoidea): a paleoenvironmental reconstruction of the Javelina Formation (Upper Cretaceous), Big Bend National Park, Texas; pp. 21–45 in K. Padian and M.A. Brown (eds.), The Late Cretaceous pterosaur *Quetzalcoatlus* Lawson 1975 (Pterodactyloidea: Azhdarchoidea). Society of Vertebrate Paleontology Memoir 19. Journal of Vertebrate Paleontology 41 (2, Supplement). DOI: 10.1080/02724634.2019.1593184.

## INTRODUCTION

The giant Late Cretaceous azhdarchid pterosaur *Quetzalcoatlus northropi* was among the largest animals that ever flew (Lawson, 1975a, 1975b). Fragmentary remains of azhdarchid pterosaurs are known from Cretaceous strata in North America (Estes, 1964; Padian and Smith, 1992; McGowen et al., 2002; Godfrey and Currie, 2005; Henderson and Peterson, 2006), Europe (Company et al., 1999; Buffetaut et al., 2002, 2003; Vremir et al., 2013), the Middle East (Arambourg, 1959; Lewy et al., 1992; Frey and Martill, 1996), Africa (Suberbiola et al., 2003), and Asia (Nesov, 1984, 1991a, 1991b; Cai and Wei, 1994; Averianov, 2007). The most complete and abundant specimens are, however, from the middle to late Maastrichtian Javelina Formation of Big Bend National Park in southwestern Texas, and housed in the Texas Vertebrate Paleontology Collections (TMM) collections (Fig. 1). The type specimen of *Quetzalcoatlus northropi* (TMM 41450-3) consists of a huge incomplete wing, found on Dawson Creek near the western boundary of the park (Lawson, 1975a; Langston, 1978). Numerous additional specimens of a smaller species, *Quetzalcoatlus lawsoni*, sp. nov. (Andres and Langston 2021), have been recovered from a limited area on the edge of Tornillo Flat, in the northern part of the park (Fig. 1).

Nesov (1984, 1991c) argued that azhdarchid pterosaurs, including *Quetzalcoatlus*, inhabited coastal lagoons or estuaries and were piscivorous. He compared azhdarchids to modern avian 'skimmers,' which capture fish from the water surface or from shallow depth while in flight, although there are no obvious morphological correlates supporting this hypothesis. Unlike remains of many other pterosaurs, often found in coastal marine and lagoonal sediments, the Big Bend *Quetza/coatlus* specimens occur in continental deposits 300–400 km from the Late Cretaceous shoreline (Lawson, 1975a; Blakey and Ranney, 2018). Some other, non-azhdarchid, pterosaurs are also known from continental, and even desert, deposits (e.g., Bell and Padian, 1995). As a result, the possible habitat and behavior of *Quetzalcoatlus* have been the subject of speculation and debate (e.g., Wellnhofer, 1991; Chatterjee and Templin, 2004).

Lawson (1975a) argued that the sedimentary context of *Quetzalcoatlus* remains and the structure of its cervical vertebrae suggest that, unlike many other pterosaurs, *Quetzalcoatlus* was not piscivorous. The absence of fish remains in the associated deposits and the lack of evidence for a large perennial body of water in the region have been cited in support of this argument (Lawson, 1975a; Langston, 1981). Lawson (1975a) instead likened *Quetzalcoatlus* to a vulture and proposed that it was a carrion feeder, using its long beak and neck to probe dinosaur carcasses. It lacks the hooked beak and talons of carnivorous birds, however. Langston (1981), noting extensive bioturbation in the strata associated with the remains, and the pronounced attenuation of the jaws, raised the possibility that *Quetzalcoatlus* foraged on the ground or in shallow water for burrowing molluscs or arthropods, plucking them from the substrate with its chopsticks-like beak.

Because they were so large, there has also been debate about whether 'giant' azhdarchids were flightless, or if capable of flight, what their likely power capabilities, takeoff methods, and

© 2021 Thomas M. Lehman.
This is an Open Access article distributed under the terms of the Creative Commons Attribution-NonCommercial-NoDerivatives License (http://creativecommons.org/licenses/by-nc-nd/4.0/), which permits non-commercial re-use, distribution, and reproduction in any medium, provided the original work is properly cited, and is not altered, transformed, or built upon in any way.

Downloaded From: https://bioone.org/journals/Journal-of-Vertebrate-Paleontology on 24 Apr 2024
Terms of Use: https://bioone.org/terms-of-use

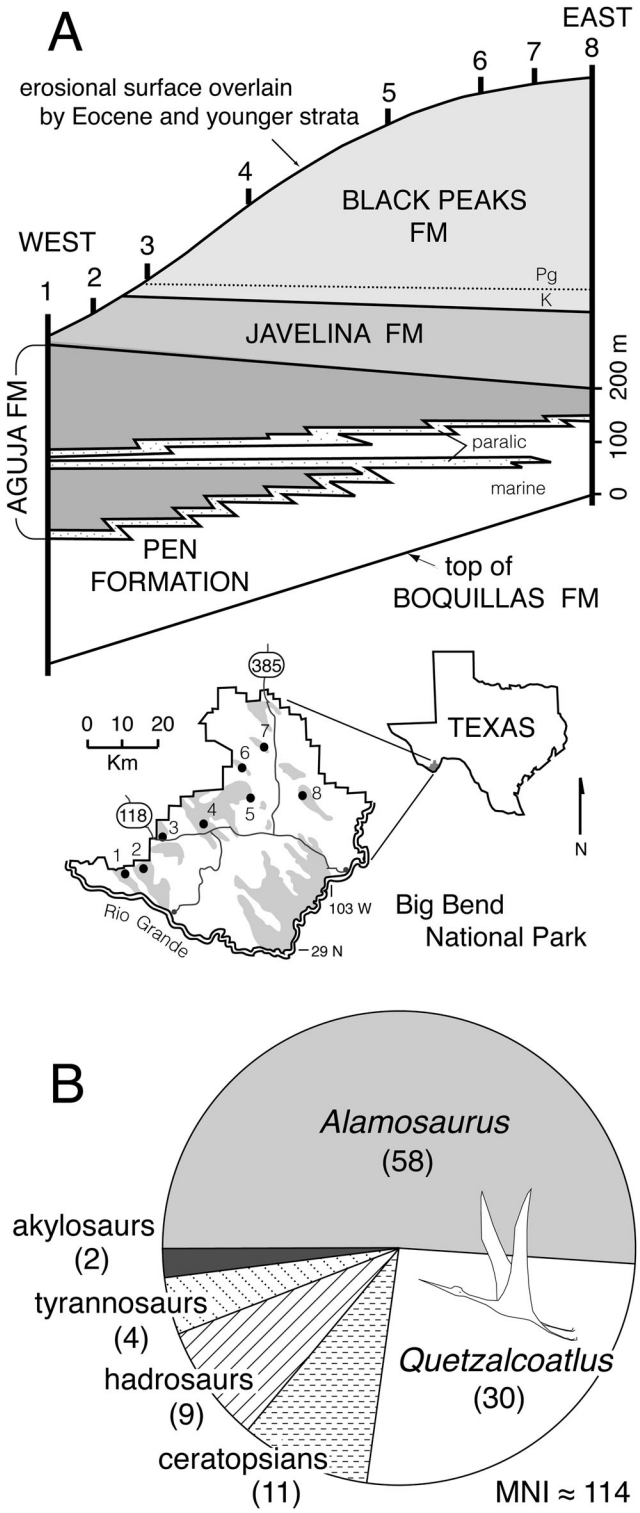


FIGURE 1. **A**, general location map and correlation diagram showing stratigraphic relationships of Upper Cretaceous and Paleocene strata in Big Bend National Park of southwestern Texas, positions of measured sections (1–8) and Cretaceous-Paleogene (K-Pg) boundary. **B**, pie diagram showing large vertebrate faunal composition of the Javelina Formation based on survey of specimens in all known museum collections. Section locations: **1**, Sierra Aguja; **2**, Pena Mt.; **3**, Dawson Creek; **4**, Paint Gap Hills; **5**, Grapevine Hills; **6**, Tornillo Flat; **7**, 'Pterodactyl Ridge'; **8**, McKinney Hills. **Abbreviation**: **MNI**, minimum numbers of individuals represented (in parentheses).

flight characteristics might have been (e.g., Witton and Habib, 2010). In cases where both 'giant' and smaller species appear to have coexisted, there is conjecture as to how they may have partitioned ecological resource zones (Vremir et al., 2013). All of these subjects of speculation can benefit from documentation of the environmental context of the pterosaur-bearing sites.

The present study documents the stratigraphic distribution of *Quetzalcoatlus* collection sites within the Javelina Formation (Fig. 2), the sedimentary facies at the localities, and provides a reconstruction of the depositional setting of these localities. In particular, a detailed account is given of the north Tornillo Flat *Quetzalcoatlus* localities, which lie along an outcrop informally termed 'Pterodactyl Ridge' (Fig. 3). Sedimentary facies analysis, petrographic and isotopic study of the pterosaur-bearing deposits, and an evaluation of the associated ichnofauna, invertebrate fauna, and flora of this interval are synthesized with taphonomic observations to yield a paleoenvironmental reconstruction. This study may help to constrain and test hypotheses about the habitat and behavior of *Quetzalcoatlus*.

## GEOLOGIC SETTING

In the Big Bend region of western Texas, Upper Cretaceous marine limestone and shale of the Boquillas and Pen formations (Cenomanian through early Campanian) grade upward into coastal deposits of the Aguja Formation (middle Campanian through early Maastrichtian) and overlying fluvial deposits of the Javelina Formation (middle to late Maastrichtian; Fig. 1A). This generally regressive depositional sequence records the retreat of the Western Interior Sea from Texas during Late Cretaceous time. The Javelina Formation is gradationally overlain by Paleocene deposits of the Black Peaks Formation, and the Cretaceous/Paleogene boundary lies just above the formation contact (Fig. 1A; Lehman, 1988, 1990; Lehman and Busbey, 2007).

These strata accumulated within the Tornillo Basin, a sedimentary basin that subsided during the Laramide Orogeny, and received sediment throughout latest Cretaceous and Paleogene time (Lehman, 1991). The Laramide-aged deposits of the Tornillo Basin, including the Javelina Formation, are predominantly of fluvial origin. Stream flow was to the southeast throughout Javelina deposition, when the coastline was 300–400 km east of the present-day Big Bend region (Fig. 4; Lawson, 1975a; Blakey and Ranney, 2018). The Javelina Formation is typically about 140 m thick but varies from 120 to 200 m, generally thickening eastward into the structurally deepest part of the Tornillo Basin, which experienced the highest rates of subsidence (Lehman, 1991).

In addition to *Quetzalcoatlus northropi*, the Javelina Formation contains a diverse fauna dominated by the sauropod dinosaur *Alamosaurus sanjuanensis* (Fig. 1B; Lawson, 1972, 1976; Lehman and Coulson, 2002; Fronimos and Lehman, 2014; Tykoski and Fiorillo, 2016). The horned dinosaurs *Bravoceratops polyphemus* (Wick and Lehman, 2013) and *Torosaurus* cf. *T. utahensis* (Hunt and Lehman, 2005), hadrosaurs (Lehman et al., 2016), and ankylosaurs are also present (Langston et al., 1989; Lehman, 1996). ?*Tyrannosaurus* sp. (Lawson, 1976; Carpenter, 1990; Wick, 2014) and several small theropods are represented by limited material. Standhardt (1986) reported a variety of fishes, smaller reptiles (turtles and crocodilians), and mammals. The presence of *Torosaurus* and ?*Tyrannosaurus* suggests that the upper part of the formation is correlative with Lancian strata, and a U-Pb isotopic age of 69 ± 0.9 Ma for a tuff bed in the middle of the Javelina Formation indicates a middle to late Maastrichtian age (Fig. 2; Lehman et al., 2006; see also Lawson, 1976; Lehman, 1987). Magnetostratigraphy suggests that the upper part of the formation (that part yielding all diagnostic remains of *Quetzalcoatlus*) is correlative with

Downloaded From: https://bioone.org/journals/Journal-of-Vertebrate-Paleontology on 24 Apr 2024
Terms of Use: https://bioone.org/terms-of-use

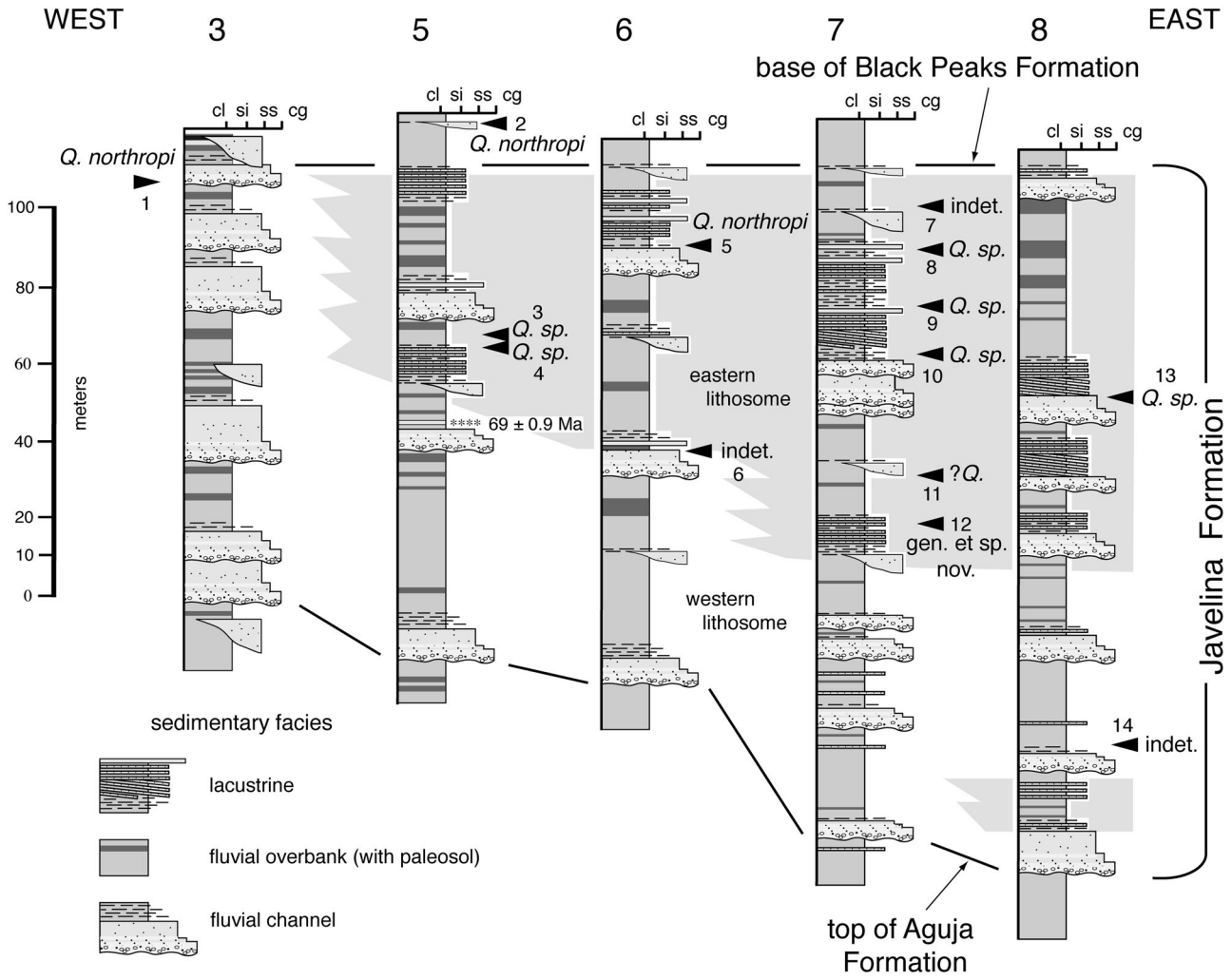


FIGURE 2. Stratigraphic sections showing distribution of three major sedimentary facies in the Javelina Formation (fluvial channel, overbank floodplain, and lacustrine) and positions of collection sites for specimens referred to *Quetzalcoatlus lawsoni*, sp. nov., *Q. northropi*, and *Wellnhopterus brevirostris*, gen. et sp. nov. (Andres and Langston 2021). Numbers 3–8 for stratigraphic sections refer to locations shown on Figure 1; 'Pterodactyl Ridge' sites are those shown on section 7; radiometric age of tuff bed on section 5 is from Lehman et al. (2006). Numbers associated with pterosaur specimens refer to the following TMM localities: **1**, 41450; **2**, 44036; **3**, 45616; **4**, 45616; **5**, 41047, 41398; **6**, 41398; **7**, 41839; **8**, main quarry level (see Fig. 7); **9**, 41961; **10**, 42272; **11**, 42889; **12**, 42489; **13**, 45888; **14**, 42538.

chron C29r and if so, is latest Maastrichian in age (ca. 67 to 66 Ma; Leslie et al., 2018).

The Javelina Formation varies in thickness and sedimentary facies geographically (Lehman, 2007). Eastern exposures of the formation are thicker, generally drab in color, and include significant lacustrine deposits (Fig. 2, 'eastern lithosome'). In western exposures, the formation is thinner, brightly colored due to well-developed paleosol horizons, and generally lacks lacustrine facies (Fig. 2, 'western lithosome'). Although indeterminate pterosaur specimens are found throughout the vertical extent of the Javelina Formation, identifiable *Quetzalcoatlus* specimens are restricted to the upper half of the formation and locally they are the most abundant component of the vertebrate fauna (Fig. 2). The lowermost diagnostic azhdarchid pterosaur specimen thus far recovered from the formation (TMM 42489-2) is a fragmentary skull with cervical vertebrae belonging to *Wellnhopterus brevirostris*, gen. et sp. nov. (Kellner and Langston, 1996; Andres and Langston, 2021). Specimens referable to *Quetzalcoatlus lawsoni*, sp. nov. (see Andres and Langston, 2021), are found throughout the upper part of the Javelina Formation. The holotype of *Quetzalcoatlus northropi* (TMM 41450-3) was found near the top of the formation, and other specimens likely referable to the species (TMM 41047-1, a femur; TMM 41398-3 and TMM 41398-4, fragments of femur and phalanx; TMM 44036-1, a fragmentary ulna) were also found in the uppermost part of the Javelina or base of the overlying Black Peaks Formation. Other 'giant' but indeterminate pterosaur bones (TMM 41839-2 to TMM 41839-12, fragments of phalanx and metatarsals) are also known only from the Javelina-Black Peaks contact interval; the only exception being a single isolated cervical vertebra (TMM 42889-1), which is tentatively referred to *Q. northropi*. Hence, the three species may succeed one another stratigraphically. Given imprecise regional stratigraphic correlation and few diagnostic specimens, it is possible that the ranges of at least the two species of *Quetzalcoatlus* overlap; however, the two have not been found together at the same sites. It is therefore uncertain whether the two *Quetzalcoatlus* species were truly contemporaneous. If they did coexist, the two species may have occupied separate habitats; their remains are typically found in separate sedimentary facies (see below).

Downloaded From: https://bioone.org/journals/Journal-of-Vertebrate-Paleontology on 24 Apr 2024
Terms of Use: https://bioone.org/terms-of-use

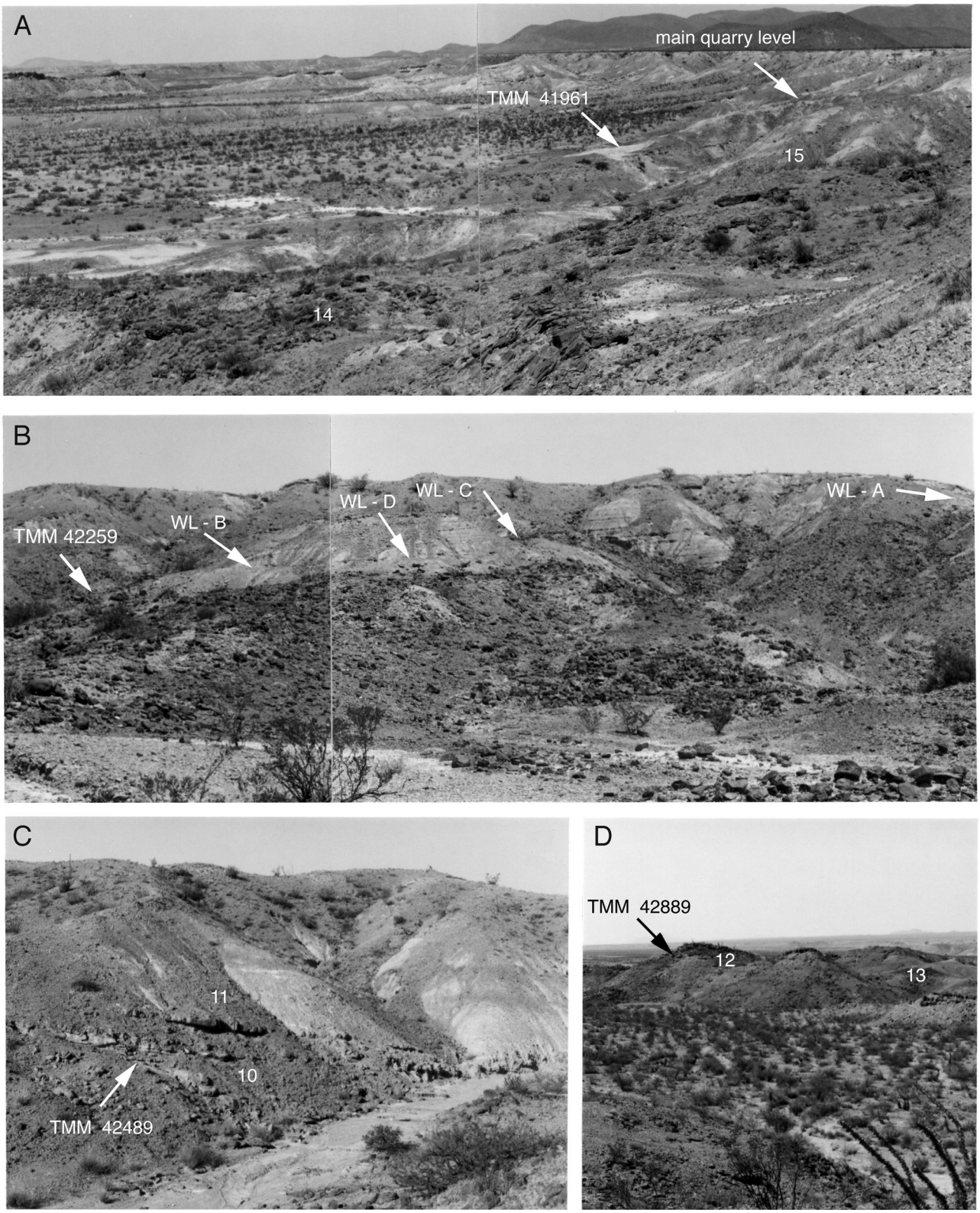


FIGURE 3. Outcrops of the Javelina Formation at 'Pterodactyl Ridge' showing **A**, view to northwest showing stream channel facies (Fig. 5, unit 14) overlain by channel-lake facies (unit 15) with *Quetzalcoatlus* collection sites; **B**, view to north showing *Quetzalcoatlus* collection sites in channel-lake facies (unit 15) along the main quarry level at Amaral Site (WL-A to WL-D and TMM 42259); **C**, view to southwest of *Quetzalcoatlus* collection site (TMM 42489) in channel-lake facies (unit 10) overlain by floodplain facies (unit 11); **D**, view to southeast of *Quetzalcoatlus* collection site (TMM 42889) in stream channel facies (unit 12) overlain by floodplain facies (unit 13).

Downloaded From: https://bioone.org/journals/Journal-of-Vertebrate-Paleontology on 24 Apr 2024
Terms of Use: https://bioone.org/terms-of-use

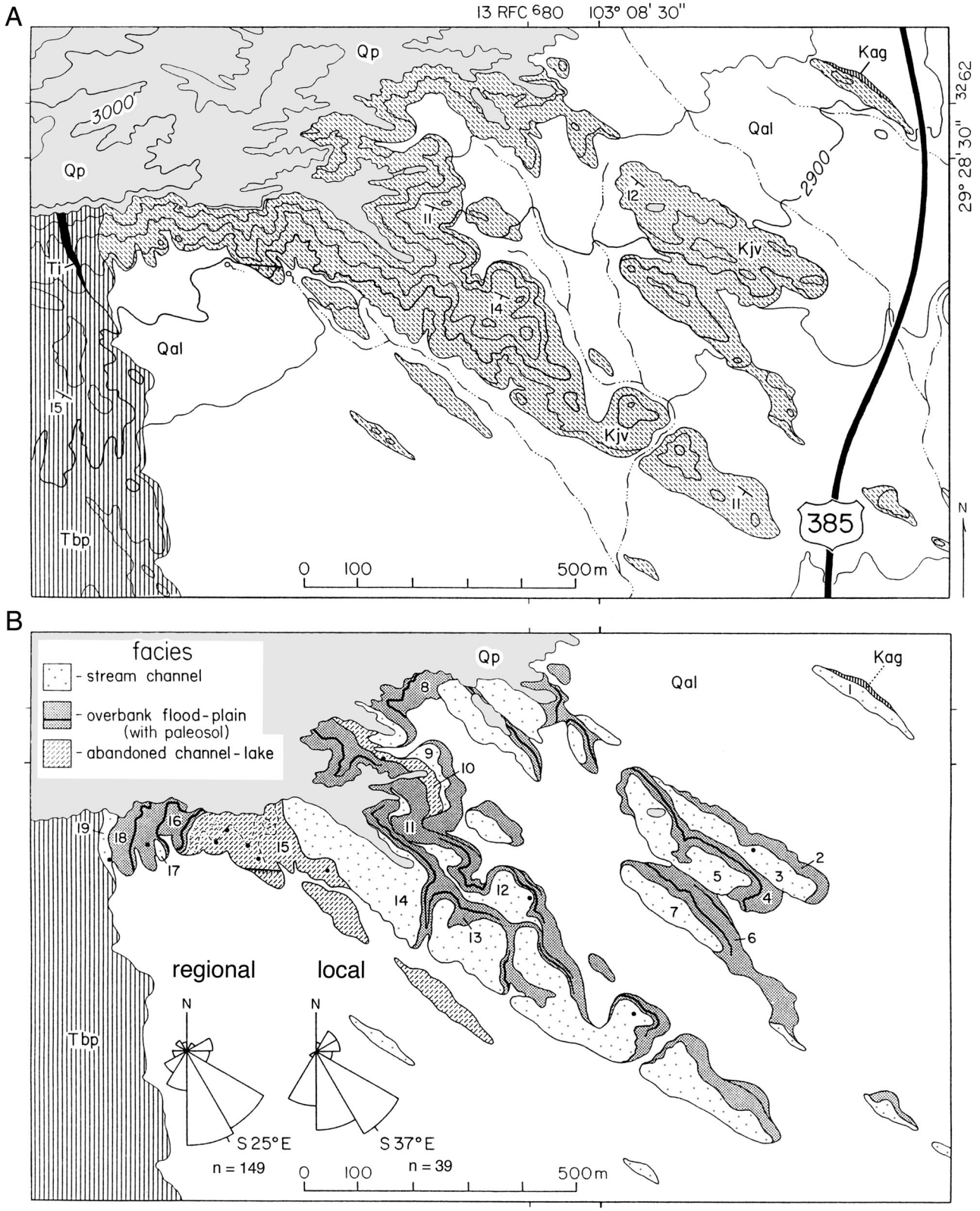


FIGURE 4. Maps showing **A**, geologic units and **B**, sedimentary facies of the 'Pterodactyl Ridge' area on north Tornillo Flat (location 7 in Fig. 1). Geologic map shows outcrops of Aguja Formation, Javelina Formation, Black Peaks Formation, Paleogene intrusive rocks, and areas covered by pediment gravel and alluvium. Numbers (1–19) on facies map refer to stratigraphic units in measured section of the Javelina Formation shown in Figures 5 and 6, and dark circles indicate significant *Quetzalcoatlus* and other fossil collection sites shown in Figure 5. Rose diagrams compare distribution and vector mean of paleocurrent data taken from trough cross-stratification in stream channel facies locally at 'Pterodactyl Ridge' with those taken regionally in the Javelina Formation. **Abbreviations**: **Kag**, Aguja Formation; **Kjv**, Javelina Formation; **K-Tbp**, Black Peaks Formation; **Qal**, alluvium; **Qp**, pediment gravel; **Ti**, Paleogene intrusive rocks.

Downloaded From: https://bioone.org/journals/Journal-of-Vertebrate-Paleontology on 24 Apr 2024
Terms of Use: https://bioone.org/terms-of-use

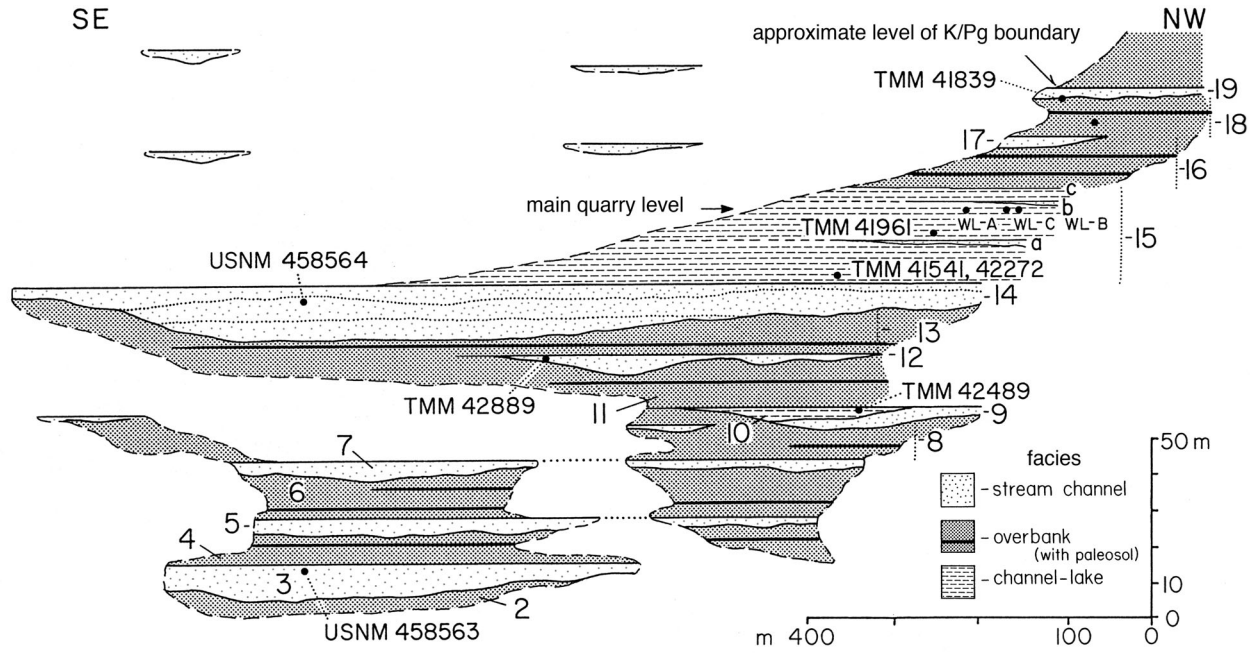


FIGURE 5. Outcrop panel diagram of 'Pterodactyl Ridge' constructed by down-dip viewing of sedimentary facies map (Fig. 4B) and scaling with measured section (Fig. 6). Numbers (2–19) refer to stratigraphic units in measured section of the Javelina Formation (Fig. 6). Major *Quetzalcoatlus* sites and other selected fossil localities are indicated (e.g., U.S. National Museum (USNM) sites are paleobotanical collections; Wheeler et al., 1994). Patterns for sedimentary facies are the same as those used in Figures 4 and 6.

## PTERODACTYL RIDGE

The 'Pterodactyl Ridge' localities lie along the north side of Tornillo Flat, in a series of northwest-trending hogback ridges where the Javelina Formation is well exposed (Figs. 3, 4). The strata in this area dip gently (10°–15°) to the southwest. The formational contacts shown herein are revised following the suggestions of Lehman (1988, 1990, 2002). The contact with the underlying Aguja Formation is exposed along the northeast side of the outcrop belt. The contact with the overlying Black Peaks Formation is exposed on the southwest side of the outcrop but is covered in most places by Holocene alluvium. To the northwest, and at higher elevations, Javelina strata are covered by Pleistocene pediment gravel, whereas at lower elevations the strata are covered by Holocene alluvium, soil, and vegetation. Sandstone units in the Javelina Formation hold up resistant hogback ridges, whereas the mudstone intervals are largely covered by alluvium.

This series of hogbacks exposes the Javelina Formation in a section roughly parallel to the Late Cretaceous stream flow direction (S25°E; Fig. 4). Topographic spurs projecting from the hogbacks and several small arroyos that transect these ridges provide cross-sections perpendicular to the paleoflow direction. A series of stratigraphic sections was measured at intervals along the Pterodactyl Ridge outcrop. Individual beds were traced laterally along the outcrop to produce a facies map of this area (Fig. 4). These maps and sections were used to construct an outcrop panel diagram illustrating the relative positions of *Quetzalcoatlus* localities within this stratigraphic framework (Fig. 5).

## SEDIMENTARY FACIES

The Javelina Formation consists predominantly of lenticular conglomeratic sandstone and varicolored mudstone of fluvial origin. Three major sedimentary facies are present within the Javelina Formation along Pterodactyl Ridge. They are identified herein as (1) stream channel facies, (2) overbank floodplain facies, and (3) abandoned channel-lake facies (Figs. 4, 5). Each of these facies is described below. The section at Pterodactyl Ridge consists of 54% overbank, 27% stream

TABLE 1. Pterosaur collection sites in Big Bend National Park with their sedimentary facies associations.

| TMM site no. | Taxon | Sedimentary facies |
|---|---|---|
| 41047 | *Q. northropi* | Stream channel |
| 41398 | *Q. northropi* | Stream channel |
| 41450 | *Q. northropi* | Stream channel |
| 41544 | *Q. lawsoni* | Lacustrine |
| 41545 | *Q. lawsoni* | Lacustrine |
| 41546 | *Q. lawsoni* | Lacustrine |
| 41547 | *Q. lawsoni.* | Lacustrine |
| 41839 | *Q.* sp. indet. | Floodplain |
| 41954 | *Q. lawsoni* | Lacustrine |
| 41961 | *Q. lawsoni* | Lacustrine |
| 42138 | *Q. lawsoni* | Lacustrine |
| 42157 | *Q. lawsoni* | Lacustrine |
| 42161 | *Q. lawsoni* | Lacustrine |
| 42180 | *Q. lawsoni* | Lacustrine |
| 42246 | *Q. lawsoni* | Lacustrine |
| 42259 | *Q. lawsoni* | Lacustrine |
| 42272 | *Q. lawsoni* | Lacustrine |
| 42297 | *Q. lawsoni* | Unknown |
| 42335 | *Q. lawsoni* | Lacustrine |
| 42422 | *Q. lawsoni* | Lacustrine |
| 42462 | *Q. lawsoni* | Lacustrine |
| 42489 | *W. brevirostris* | Lacustrine |
| 42521 | *Q. lawsoni* | Lacustrine |
| 42538 | *Q.* sp. indet. | Floodplain |
| 42889 | *Q. northropi* | Stream channel |
| 44036 | *Q. northropi* | Stream channel |
| 44037 | *Q. lawsoni* | Lacustrine |
| 45616 | *Q.* sp. indet. | Lacustrine |
| 45888 | *Q. lawsoni* | Stream channel |
| 45977 | *Q. lawsoni* | Lacustrine |

Downloaded From: https://bioone.org/journals/Journal-of-Vertebrate-Paleontology on 24 Apr 2024
Terms of Use: https://bioone.org/terms-of-use

channel, and 19% abandoned channel-lake facies. The general character and abundance of these facies is comparable to that found elsewhere—at least within the eastern exposures of the Javelina Formation (Fig. 2). Western exposures of the formation largely lack the channel-lake facies (Lehman, 2007). Although pterosaur remains are found as isolated skeletal elements in the stream channel and overbank facies, the associated to partially articulated specimens are confined to the abandoned channel-lake facies (Table 1).

### Stream Channel Facies

Stream channel deposits consist of interbedded conglomerate and sandstone in lenticular units ranging between 3–10 m in thickness. Individual channel units are tabular or sheet-like in geometry and may be traced up to 2 km along strike (Figs. 4, 5). Conglomerate beds consist of granule- to cobble-size clasts of carbonate nodules, petrified wood fragments, abraded bones, and sparse chert pebbles. These clasts are predominantly of intrabasinal origin and represent the coarsest fraction of stream bed load, swept from the surrounding floodplain and accumulated in channel thalweg environments. Conglomerate beds are typically less than 1 m thick. Crude horizontal bedding and low-angle cross-bedding indicate that this gravel was deposited primarily under upper flow regime conditions. Large isolated bones found in the conglomerate beds are predominantly vertebral centra and fragments of appendicular bones of *Alamosaurus*. In places, the conglomerates contain concentrations of smaller bones, including gar vertebrae and scales, amiid fish vertebrae, crocodilian teeth and osteoderms, and turtle shell fragments. Several types of gastropod shells are also found (see below).

The sandstone beds consist of tan to light olive gray, very fine- to medium-grained feldspathic litharenite to lithic arkose (mean = $Q_{33}$ $F_{21}$ $L_{46}$, n = 9). The sand consists predominantly of quartz, volcanic rock fragments, and plagioclase derived from distant volcanic source areas to the west and northwest, probably in northern Mexico or southern New Mexico and Arizona (Lehman, 1991). The sand also contains chert, limestone fragments, and reworked Cretaceous foraminifera from nearby source areas in uplifted older Cretaceous marine strata exposed along the flanks of the Tornillo Basin. The sandstone beds exhibit prominent horizontal parallel lamination with parting lineation on bedding planes and broad trough cross-bedding in sets generally less than 30 cm in thickness (Figs. 6, 7). Thin intervals of current ripple cross-lamination are also present, generally in the upper parts of channel deposits. The uppermost parts of channel sandstone units also display extensive bioturbation (see below). Incomplete disarticulated skeletons, scattered vertebrae, and limb bones of *Alamosaurus* are relatively common in the sandstone beds, and local accumulations of transported logs with some 'log jams' of more than 20 trunks are observed (see below).

A typical vertical sequence through the stream channel facies is about 3.5 m thick and consists of a basal conglomerate resting on an erosional surface, grading upward into gently inclined beds of parallel-laminated sandstone and overlain by low-angle trough cross-bedded sandstone and thin beds of rippled and bioturbated sandstone (Fig. 7). Most sandstone intervals consist of one to three such sequences superimposed. Prominent bar accretion surfaces, gently inclined laterally and downstream, transect each channel sequence. The abundance of parallel-laminated sand, and low-angle trough cross-bedding, indicates deposition primarily under upper flow regime conditions and under conditions transitional between lower and upper flow regimes. The prominent lateral and downstream bar accretion surfaces and the absence of cosets of tabular cross-strata indicate that sediment deposition took place primarily on migrating low-relief lateral or point bars, not on mid-channel transverse bars.

The typical thickness of the stream channel facies sequence and inclination of lateral accretion surfaces allow estimation of original depth and width of the Javelina streams. Using the methods for reconstructing paleochannel morphology given by Ethridge and Schumm (1978) and Smith (1987), the maximum bankfull depth of a typical Javelina stream is estimated at 3.5 m, and the bankfull channel width at 45 m. Empirical relationships established for modern meandering streams indicate that such a stream would have a meander wavelength of 500–600 m and a radius of meander curvature of 100–200 m (Schumm, 1960). The characteristics and estimated dimensions of Javelina streams are comparable to those found in small streams that traverse the semiarid Great Plains of western U.S.A. today, and that transport alluvium containing a relatively small amount of gravel. The relatively high width/depth ratio of Javelina streams is consistent with a high percentage of silt and clay in the alluvium, as is also evident in the dominance of overbank facies in the Javelina section.

The preponderance of parallel-laminated sand in Javelina channel bar deposits indicates that flow in these streams was dominated by shallow high-velocity flood events of short duration. Stream discharge fluctuated dramatically and was perhaps even ephemeral. The steep-sided scours and caliche gravel mounds that separate bar accretion units are evidence for falling-stage modification and incision of emergent bar surfaces during periods of low flow. The features of Javelina stream channel

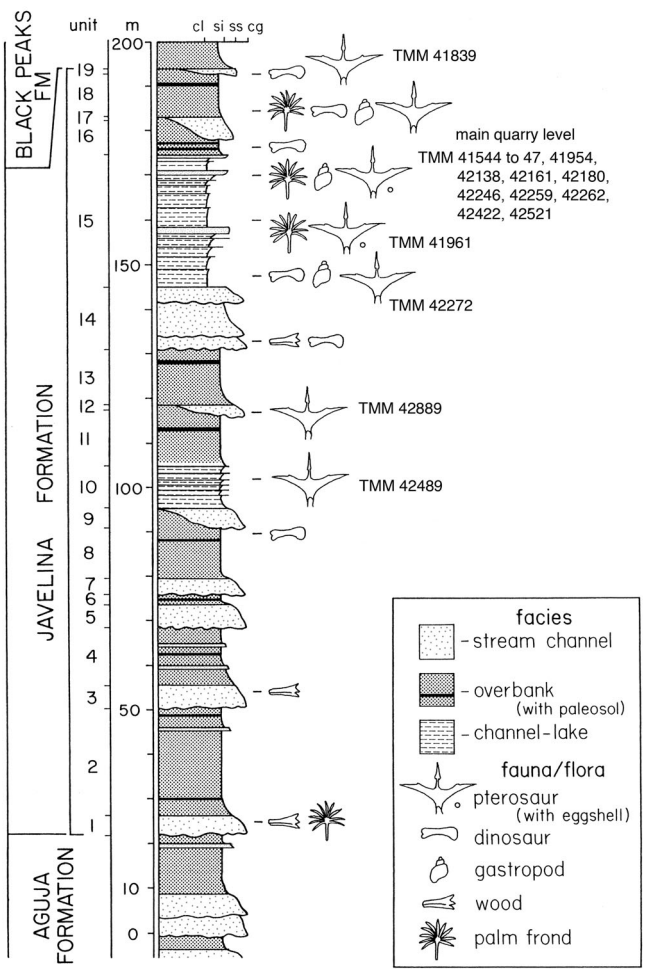


FIGURE 6. Measured section of the Javelina Formation at 'Pterodactyl Ridge' showing distribution of sedimentary facies and significant fossil collection sites. **Abbreviations**: **cg**, conglomerate; **cl**, claystone; **si**, siltstone; **ss**, sandstone.

Downloaded From: https://bioone.org/journals/Journal-of-Vertebrate-Paleontology on 24 Apr 2024
Terms of Use: https://bioone.org/terms-of-use

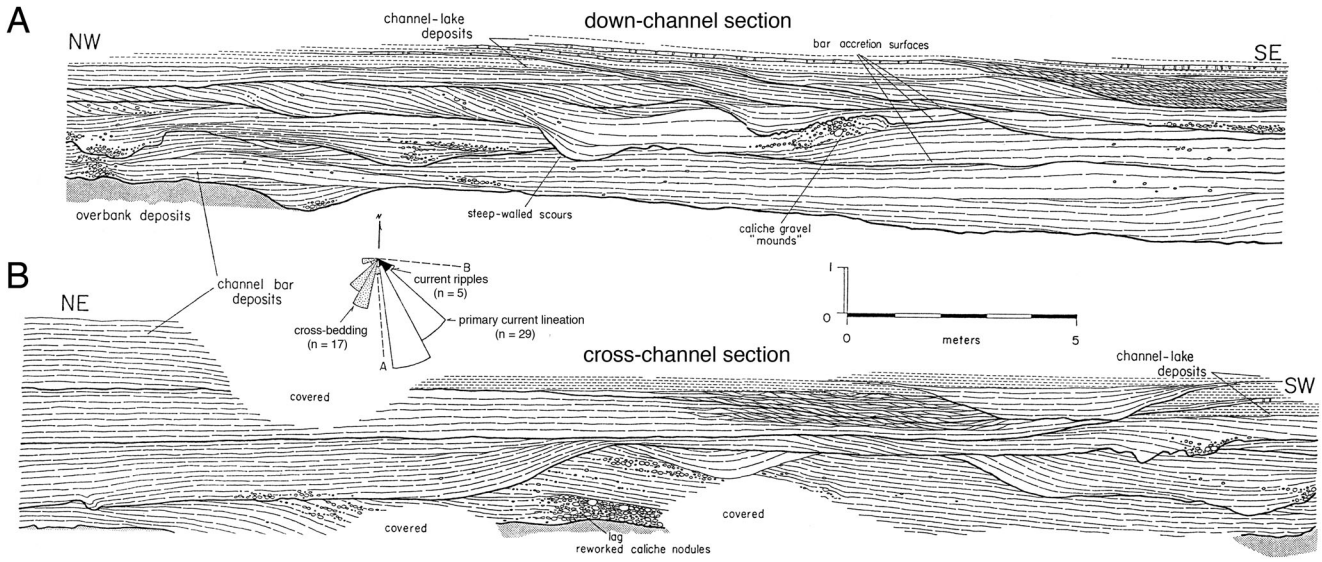


FIGURE 7. Outcrop panel diagrams of typical stream channel facies in the Javelina Formation, showing cross-sections **A**, parallel to paleocurrent direction and **B**, perpendicular to paleocurrent direction (channel unit shown at 60 m level in measured section 5 in Fig. 2). Stream channel facies rest on an erosional surface incised in underlying overbank floodplain facies and are gradationally overlain by channel-lake facies. Inset rose diagram shows orientation of sections **A** and **B** relative to paleocurrent data taken at this site from current ripple cross-lamination, trough cross-bedding, and primary current lineation (downstream direction shown).

facies are comparable to those summarized in the Bijou Creek fluvial facies model of Miall (1978). Similar present-day and ancient ephemeral stream deposits have been described by Sneh (1983), Stear (1983), Wells (1983), and Tunbridge (1984).

### Overbank Floodplain Facies

Overbank floodplain deposits consist largely of light gray to drab olive (5Y8/1, Munsell color notation) mudstone with thin intervals of red to purple (5R5/2) mudstone. These fine-grained deposits constitute most of the Javelina section and provide evidence for the high suspended sediment load of Javelina streams (Fig. 4, 5). The clays are mostly smectite and mixed-layer smectite-illite with variable amounts of silt composed of quartz and plagioclase (Lehman, 1989). Both gray and purple beds contain dispersed irregular nodules of microcrystalline calcite and in places barite, varying from 1 to 10 cm in diameter. The olive and gray mudstone intervals display crude horizontal stratification in some places; however, red and purple beds generally exhibit blocky, massive structure with fine root mottling and burrows. Thin, sheet-like beds of sandstone, generally less than 1 m thick, with parallel lamination and ripple cross-lamination, interfinger locally with the mudstone. These sheet sandstones were likely produced by crevassing and levee construction adjacent to stream channel environments.

The color, structure, and chemistry of the mudstone beds and their spatial association with accumulations of nodular micritic calcite are interpreted as a result of periodic soil development in floodplain environments (Lehman, 1989, 1990). A typical floodplain paleosol consists of surficial silty pale gray (5Y7/2) A horizon (about 1 m thick), underlain by clayey red or purple (5R5/2) B horizon (about 1 m thick), which grades downward into olive gray (5Y8/1) mudstone representing floodplain alluvium relatively unmodified by soil-forming processes (Fig. 8). Organic-rich surficial horizons are rarely preserved. Nodules of micritic calcite (calcic or petrocalcic horizons) are generally concentrated within or just below the red B horizon. Some nodules contain barite crystals and barite pseudomorphs of gypsum crystals (Lehman, 1989). The calcite nodules yield a stable carbon and oxygen isotopic signature compatible with their origin by soil-forming processes (Ferguson et al., 1991; Nordt et al., 2003; Schmidt, 2009; see below). The varied development of these petrocalcic horizons, and the varied accumulation of illuvial clay and iron, indicates that the paleosols differ in maturity both stratigraphically and regionally (Lehman, 1989; Atchley et al., 2004). Many of the paleosols are weakly differentiated and similar to modern alluvial Inceptisols or Entisols (e.g., Retallack, 1983; Mack et al., 1993); this is particularly the case in eastern exposures of the Javelina Formation (Fig. 2, 'eastern lithosome'). Mature paleosols are more extensive in western exposures of the formation (Fig. 2, 'western lithosome'); these are well differentiated and similar to modern Alfisols of subhumid to semiarid regions, which support deciduous forest or savanna (Lehman, 1990; Atchley et al., 2004).

Occurrence of fossilized bone is rare in the overbank floodplain facies. Where present, bones are generally coated with a thin layer of iron oxide and a thick crust of nodular or fibrous calcite. Highly weathered fragments of sauropod limb bones, ribs, and vertebrae are the most common elements preserved. Locally the floodplain facies contains fallen logs and branches riddled with termite borings, and at several localities stumps are preserved in life position (Wheeler and Lehman, 2000; see below).

These deposits record accumulation of suspended sediment by flooding in overbank floodplain environments adjacent to stream channels. Extended periods of soil development occurred when floodplain sedimentation slowed, perhaps during episodes of channel incision or avulsion of nearby stream courses. Similar ancient floodplain sequences have been described by Bown and Kraus (1981) and Retallack (1983).

### Abandoned Channel-Lake Facies

The abandoned channel-lake facies is the least common of the three (5Y8/1) recognized in the Javelina Formation. This facies

Downloaded From: https://bioone.org/journals/Journal-of-Vertebrate-Paleontology on 24 Apr 2024
Terms of Use: https://bioone.org/terms-of-use

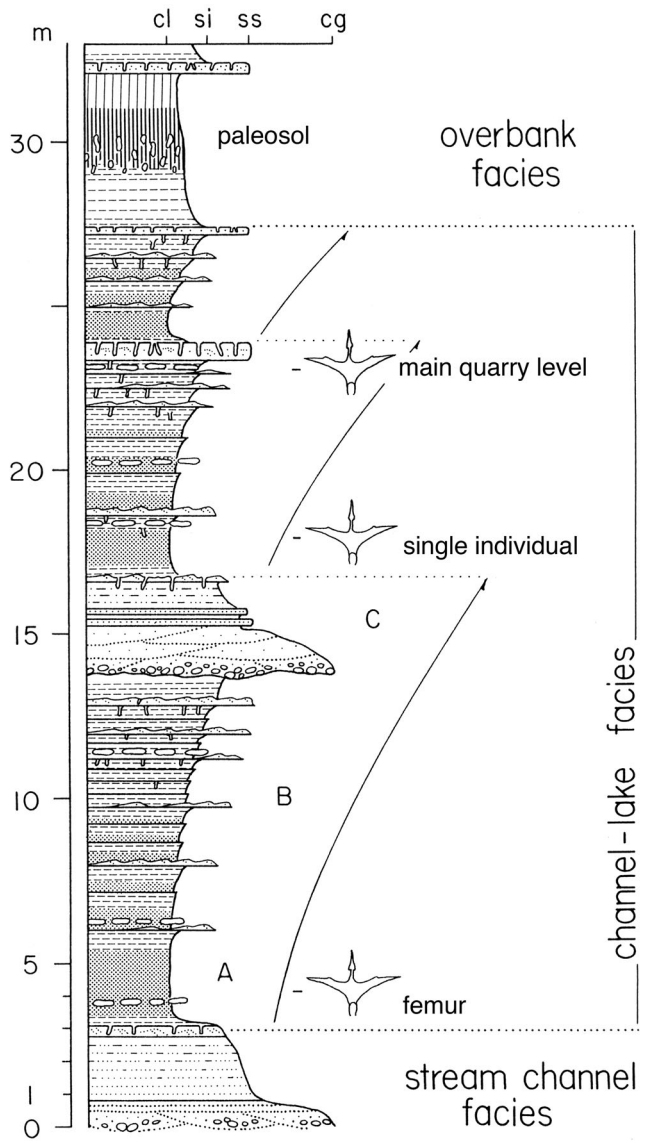


FIGURE 8. Detailed measured section of abandoned channel-lake facies (unit 15 in Fig. 6) at 'Pterodactyl Ridge' showing three coarsening-upward cycles (indicated with arrows) and three successive subfacies (A, B, C) within each cycle. Channel-lake facies here are gradationally overlain by overbank floodplain facies and underlain by stream channel facies. **Abbreviations**: **cg**, conglomerate; **cl**, claystone; **si**, siltstone; **ss**, sandstone.

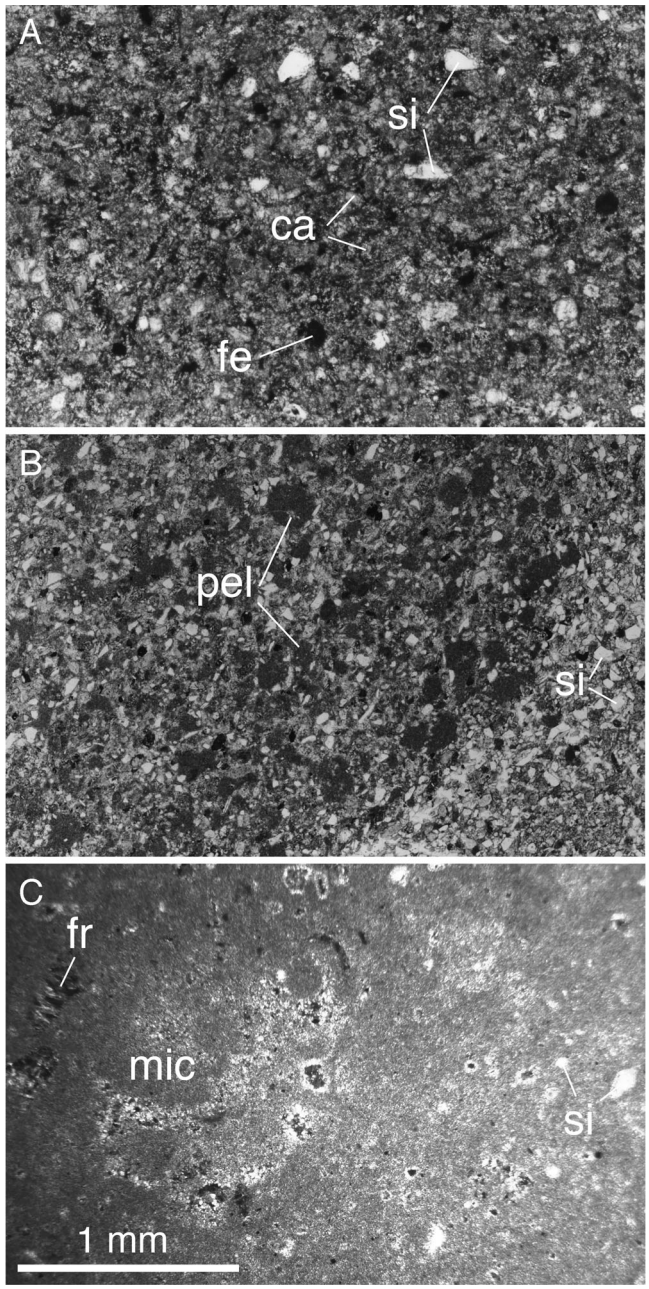


FIGURE 9. Thin-section photomicrographs (in cross-polarized light) showing lithology of channel-lake facies at 'Pterodactyl Ridge' from upper coarse-grained to lower fine-grained intervals. **A**, sandy calcareous siltstone with quartz and feldspar grains, calcite silt grains, and iron oxide grains (replacement of pyrite); **B**, burrowed calcareous siltstone with micrite pelloids partially filling burrow (left) in fine quartz and calcite silt; **C**, silty micritic mudstone showing clotted microcrystalline calcite matrix with scattered bone fragments and quartz silt grains. **Abbreviations**: **ca**, calcite silt grains; **fe**, iron oxide grains; **fr**, bone fragments; **mic**, clotted microcrystalline calcite matrix; **pel**, micrite pelloids; **si**, quartz.

consists of rhythmically interbedded drab olive green to gray (5GY6/1) calcareous claystone and nodular argillaceous limestone, tan (10YR7/2) bioturbated siltstone, and very fine sandstone. These lacustrine deposits form lenticular units 5–10 m thick, locally superimposed to produce composite sections more than 20 m thick. This facies is spatially associated in all instances with underlying stream channel deposits (Figs. 5–7). This relationship is particularly evident at TMM locality 42489 on Pterodactyl Ridge (Fig. 5). In some areas, the abandoned channel-lake facies extend beyond the limits of underlying channel deposits. Thin sequences of this facies are found within the upper part of most stream channel deposits, where less than 1 m may be present. Such an association suggests that these sediments accumulated in environments developed during the later stages of aggradation within stream channels, during and following channel abandonment by avulsion or cut off from active flow. These deposits may be distinguished from surrounding and overlying overbank facies by their high carbonate content, drab color, prominent rhythmic stratification, intercalated thin sandstone beds, and abundance of bioturbation.

Typically, the abandoned channel-lake facies comprise coarsening-upward cycles, with three successive subfacies (units A, B, and

Downloaded From: https://bioone.org/journals/Journal-of-Vertebrate-Paleontology on 24 Apr 2024
Terms of Use: https://bioone.org/terms-of-use

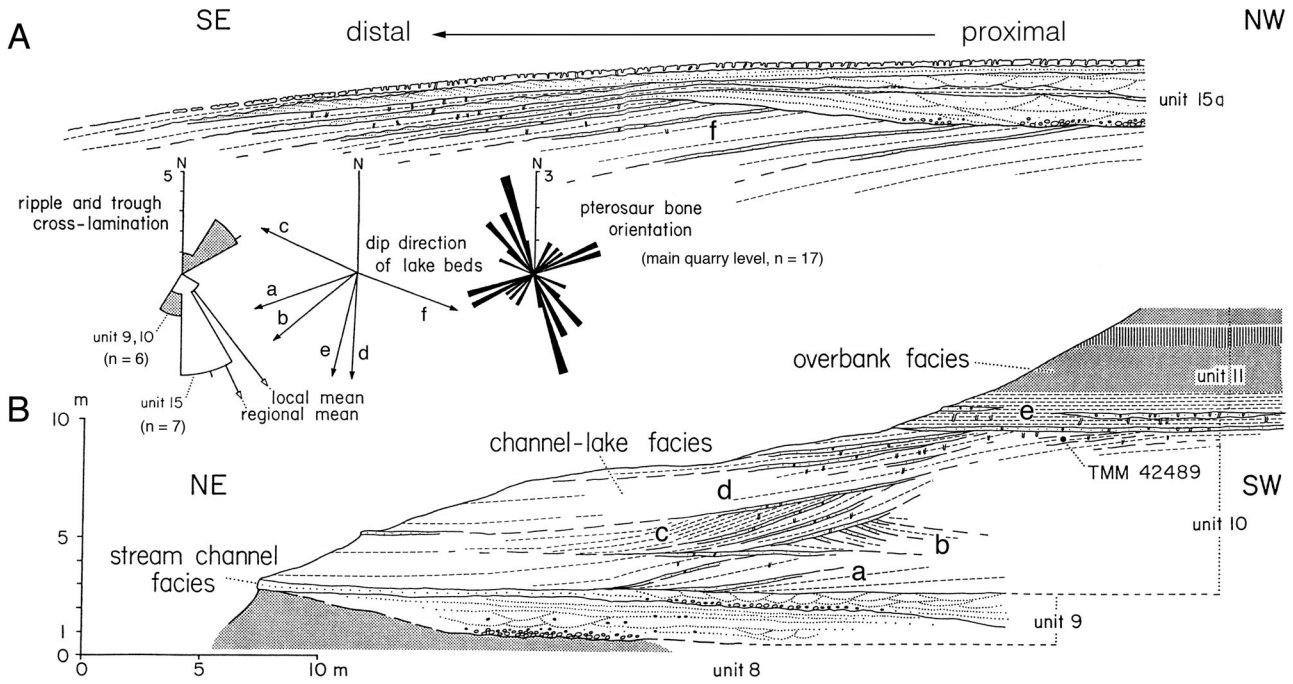


FIGURE 10. Outcrop panel diagrams of abandoned channel-lake facies at 'Pterodactyl Ridge' showing **A**, inferred near channel (proximal) to open lake (distal) gradation within lower cycle of unit 15; and **B**, discordant stratigraphic relationships among subunits (**a**–**e**) in unit 10 and relationship to underlying stream channel facies (unit 9) and overlying overbank floodplain facies (unit 11). Inset rose diagrams show paleocurrent data (ripple and trough cross-stratification) taken from channel-lake facies, dip direction of inclined stratification in channel-lake deposits (**a**–**f**), and orientation of pterosaur long bones relative to local and regional vector mean stream flow directions taken from stream channel facies (see Fig. 4).

C in Fig. 8). The basal part of a cycle (unit A) consists of 1–3 m of massive, brecciated olive gray calcareous claystone and nodular argillaceous limestone (Fig. 9). The claystone and nodular limestone grade upward into a middle interval (unit B) composed of 1–8 m of rhythmically interbedded calcareous siltstone and very fine sandstone. The thin beds of siltstone and sandstone are parallel-laminated and ripple cross-laminated with disseminated carbonized plant fragments on bedding planes. The siltstone-sandstone interbeds form couplets varying from less than 10 cm to over 1 m in thickness, coarsening and thickening upward. Burrows are distributed throughout this part of the section. Both claystone and interbedded siltstone units are highly calcareous (Fig. 9; 10–20 wt% calcium carbonate). Silt grains consist predominantly of microcrystalline calcite clasts, detrital subhedral rhombic or polyhedral calcite crystals, and biogenic calcite spherules (probably algal or microbial in origin). Indeed, much of this carbonate sediment is likely of biogenic origin. These beds also contain stratiform accumulations of calcite concretions and cross-cutting fractures filled with calcite. The concretions and fracture fillings have a distinctive radial fibrous crystal structure, differing from the nodular micritic calcite typically found in overbank floodplain facies. Bones found in this part of a cycle are generally encrusted by this form of calcite (see below).

Each cycle is typically capped by a lenticular fine sandstone bed, 0.5–3 m thick (unit C). Where traced along strike, these lenticular sandstone units thin and pinch out within the rhythmically bedded claystone and siltstone (Fig. 10). At their thickest points, the sandstone beds rest on an erosional surface mantled with conglomeratic lag of reworked carbonate nodules and incised into the underlying claystone/siltstone beds. The conglomerate grades upward into trough cross-bedded fine sandstone. Sets of cross-strata are separated by drapes of silty claystone. The cross-stratified beds grade upward into parallel-laminated very fine sandstone and siltstone capped by an interval of current-rippled and bioturbated siltstone. This capping unit weathers to a dark reddish brown color (10YR4/2) and is better cemented than the underlying tan sandstone—and so makes a convenient marker bed. The capping sandstone thins along strike and is gradually replaced by parallel-laminated and ripple cross-laminated siltstone. Traced further, the unit continues to thin, becomes concretionary, and grades entirely to ripple cross-laminated and bioturbated siltstone. Impressions of palm fronds occur within this unit.

Stratification within the abandoned channel-lake facies is gently inclined (up to 10°) relative to underlying channel deposits. Where several cycles are superimposed, they dip at slightly different angles. Internal stratification within a cycle is also subtly discordant, with bed sets inclined in different directions (Fig. 10). The inclined bedding is concordant with, at angles to, or counter to the stream paleoflow direction in underlying channel deposits (Fig. 10). The three cycles evident in the area of the main quarry on Pterodactyl Ridge each thin successively upward, and the outcrop transects each at a successively more distal depositional position.

The drab color, preservation of carbonized plant material, and abundant bioturbation indicate that deposition of this facies took place under subaqueous conditions. The thick, massive claystone and nodular limestone in the base of each cycle suggests that stagnant or very low current velocities initially prevailed in this environment. The cyclic alternation of claystone and siltstone, and clay drapes in the sandstone interval that caps each cycle, indicates that sediment deposition was episodic. The discordant angular relationships between cycles and within cycles suggest longer-term periodic deposition. The absence of evidence for soil development (oxidation, root mottling, nodular micritic carbonate), absence of wood, and good preservation of primary stratification features indicate that this environment was neither vegetated nor subaerially exposed for prolonged periods. The fine texture of the sediment, and the paleocurrent evidence that suggests low-velocity flow at

Downloaded From: https://bioone.org/journals/Journal-of-Vertebrate-Paleontology on 24 Apr 2024
Terms of Use: https://bioone.org/terms-of-use

angles to, or in opposition to, the prevailing stream flow direction, indicates that this environment did not receive sediment through normal channelized stream flow. However, the spatial association of these deposits with underlying stream channel facies requires that their origin is related in some way to channel environments.

Thus, the channel-lake facies is interpreted as the deposits of small lakes developed within abandoned reaches of stream channels. Sediment accumulated in standing water within these lakes and, periodically, by overbank flooding from nearby active streams. The abundant biogenic carbonate in these deposits is similar to that precipitated by the photosynthetic activities of algae and microbes in present-day alkaline lakes (Kelts and Hsu, 1978; Gerdes et al., 1994). The cyclic coarsening-upward intervals indicate that the lakes filled as a result of episodic progradation by crevassing or natural levee migration from nearby active channels. The lakes were likely no more than several hundred meters wide and at most only a few meters deep during their maximum extent. The main fossiliferous level on Pterodactyl Ridge is unusual in recording a prolonged period of lake development. A similar depositional system, from a cooler and more humid environment however, has been described in the avulsion belt of today's Saskatchewan River in Canada (Smith and Perez-Arlucea, 1994).

## ISOTOPE GEOCHEMISTRY

Nodules of microcrystalline calcite are found throughout the paleosols of the overbank floodplain facies (Lehman, 1989). These provide information about the local climate during deposition of the Javelina Formation. Such carbonate accumulations (caliche, calcrete, calcic, or petrocalcic horizons of authors) are generally restricted to soils in arid or semiarid climates, where annual rainfall is typically less than about 1 m (Cerling, 1984; Cerling and Hay, 1986). The stable carbon and oxygen isotopic composition of soil-formed calcium carbonate is governed by the carbon isotopic ratio in vegetation growing at the soil surface (i.e., the proportions of plants following C3 and C4 photosynthetic pathways) and by the oxygen isotopic ratio in precipitation received by the soil (Cerling, 1984). Both carbon and oxygen isotopic ratios are related to mean annual temperature (Cerling, 1984).

Samples of carbonate nodules from Javelina paleosols were analyzed to determine their stable carbon and oxygen isotopic ratios (Fig. 11; Table 2). Some of these analyses were presented by Ferguson et al. (1991). Eight samples (one sample per paleosol) were collected from successive paleosols in two sections of the Javelina Formation. The data are consistent with precipitation of the nodules in a soil environment and are compatible with modern soil-formed carbonates. The stable carbon isotopic ratio ($^{13}C/^{12}C$, measured as $\delta^{13}C$ relative to Pee Dee Belemnite [PDB] standard) varies from −8.37‰ to −9.76‰ (mean = −9.16‰), consistent with the dominance of C3 vegetation on Javelina soils. Similar isotopic values were reported for Javelina pedogenic carbonates by Nordt et al. (2003) and Schmidt (2009). The oxygen isotopic ratio ($^{18}O/^{16}O$, measured as $\delta^{18}O$ relative to PDB standard) varies from −2.27‰ to −4.82‰ (mean = −4.11‰), implying precipitation from meteoric water with $\delta^{18}O$ versus standard mean ocean water (SMOW) of 0‰ to −5‰, assuming a reasonable range of soil temperature. This range of values correlates with a mean annual air temperature exceeding 15°C (Cerling, 1984; Gregory et al., 1989). Although correlation of $^{18}O/^{16}O$ ratio in precipitation with mean annual temperature is poor for temperatures exceeding 15°C, the suggested correlation given by Cerling (1984:fig. 4), ignoring any 'monsoon effect,' implies mean annual temperatures in the range of 20–30°C for the Javelina paleosols. Based on similar observations, Dworkin et al. (2005) and Schmidt (2009) estimated that mean annual temperature fluctuated between 16°C and 23°C during deposition of the Javelina Formation.

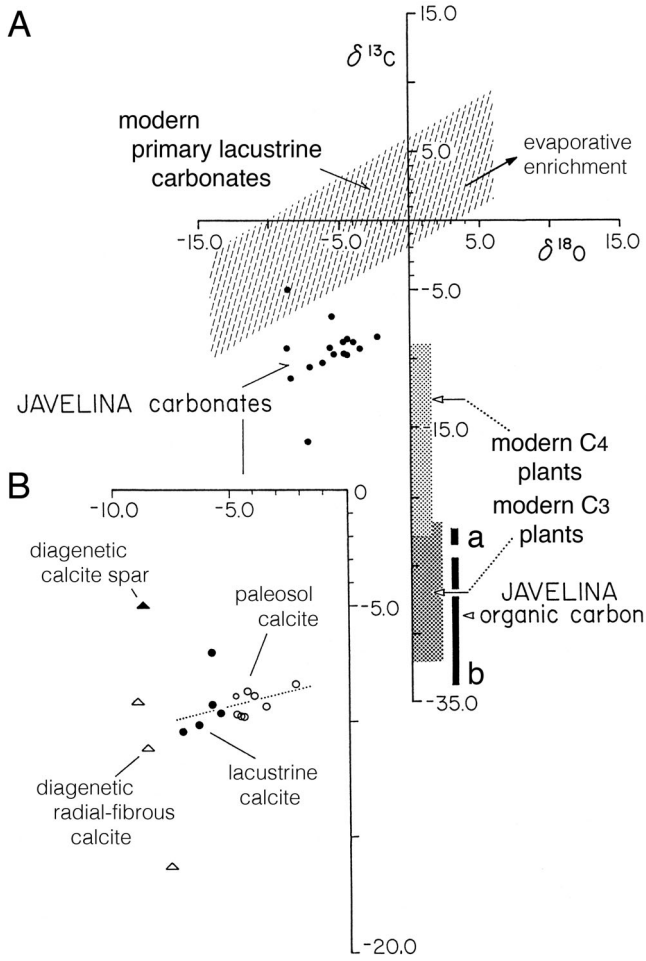


FIGURE 11. Stable carbon and oxygen isotopic ratios for carbonates and organic matter from the Javelina Formation (see Table 2). **A**, bivariate plot showing the typical range in stable carbon and oxygen isotopic ratios found in primary lacustrine carbonates of modern lakes (stippled area), and enrichment trend with evaporation (from Talbot and Kelts, 1990), compared with carbonate samples taken from the Javelina Formation (dark circles). The typical range in stable carbon isotopic ratios found in modern C4 and C3 plants (from Cerling, 1984) is compared with that found in organic carbon extracted from **a**, channel-lake facies and **b**, overbank floodplain facies in the Javelina Formation. **B**, detailed bivariate plot of isotopic ratios in Javelina carbonates showing isotopic enrichment in calcite of paleosol petrocalcic nodules relative to microcrystalline calcite in lacustrine sediment. Isotopic ratios in radial-fibrous and sparry calcite, clearly of diagenetic origin, are outside the range for primary lacustrine and paleosol carbonate. Carbon and oxygen isotopic values are reported using delta (δ) notation in permil (‰) units relative to the international Vienna PDB standard. An in-house laboratory standard calibrated relative to NBS-19 was used, with an overall precision ± 0.1‰ and ± 0.2‰ for carbon and oxygen, respectively.

Isotopic analyses of the carbonate sediment and concretions surrounding the pterosaur bones yield information about water conditions in the abandoned channel lakes (Fig. 11). Five samples of detrital silty micrite sediment, as well as laminated micrite coatings from the interior and exterior of bones, represent primary lacustrine carbonate. These samples have $\delta^{13}C$ values (−7‰ to −10‰ PDB) comparable to that found in the paleosol carbonate nodules. This suggests that the catchment area for the lakes (i.e., the drainage basin of the river) was well vegetated. In this case, lacustrine carbonate, like soil-formed carbonate, reflects a carbon isotopic composition influenced primarily by

Downloaded From: https://bioone.org/journals/Journal-of-Vertebrate-Paleontology on 24 Apr 2024
Terms of Use: https://bioone.org/terms-of-use

TABLE 2. Stable carbon and oxygen isotopic data for carbonates and organic matter from the Javelina Formation.

| Carbonate | $\delta^{13}C$ | $\delta^{18}O$ |
|---|---|---|
| Paleosol microcrystalline calcite nodules | | |
| DC-1 | −9.31 | −3.49 |
| DC-2 | −8.68 | −4.30 |
| DC-3 | −9.73 | −4.65 |
| DC-4 | −8.89 | −3.99 |
| DO-1 | −9.76 | −4.55 |
| DO-2 | −8.86 | −4.82 |
| DO-3 | −8.37 | −2.27 |
| DO-4 | −9.66 | −4.77 |
| Lacustrine micritic calcite sediment | | |
| JV-16 | −7.02 | −5.80 |
| JV-16 | −7.02 | −5.80 |
| JV-15 | −10.14 | −6.39 |
| Lacustine micritic calcite, internal sediment within bones | | |
| TM-41 | −9.61 | −5.43 |
| TM-42 | −9.26 | −5.79 |
| JV-11 | −10.40 | −7.06 |
| Early diagenetic radial fibrous calcite, fracture filling and bone coating | | |
| JV-18 | −9.12 | −8.99 |
| TM-41a | −11.15 | −8.56 |
| TM-42b | −16.25 | −7.63 |
| Late diagenetic equant calcite spar | | |
| TM-42c | −4.92 | −8.73 |
| Carbon | $\delta^{13}C$ | |
| Floodplain mudstone, particulate organic matter | | |
| PM-1a | −24.59 | |
| PM-1c | −33.54 | |
| PM-1d | −28.48 | |
| PM-2a | −26.50 | |
| PM-2b | −27.05 | |
| PM-2c | −33.06 | |
| GH-11 | −30.63 | |
| GH-13 | −31.69 | |
| GH-16 | −25.32 | |
| FW-3 | −25.80 | |
| FW-9a | −27.98 | |
| FW-14 | −33.81 | |
| FW-20a | −24.69 | |
| MR-37a | −27.79 | |
| MR-37c | −29.43 | |
| Lacustrine mudstone, particulate organic matter | | |
| JV-17 | −23.32 | |
| JV-20 | −22.39 | |
| JV-23 | −23.54 | |
| JV-28 | −23.32 | |

Carbon and oxygen isotopic values are reported using delta (δ) notation in permil (‰) units relative to the international Vienna PDB standard. An in-house laboratory standard calibrated relative to NBS-19 was used, with an overall precision ± 0.1‰ and ± 0.2‰ for carbon and oxygen, respectively.

the decomposition of isotopically light terrestrial plant material. However, $\delta^{18}O$ values for primary lacustrine carbonate are 1‰ to 2‰ lighter than paleosol carbonates. Schmidt (2009) found similar isotopic differences between Javelina paleosol and lacustrine carbonates. Because soil water loss through transpiration by plants is nonfractionating, this may indicate that soil waters were slightly enriched by evaporation compared with river or lake water (Cerling, 1984). Occasional strong evaporation of soil water is indicated by pseudomorphically replaced gypsum crystals in some paleosol carbonate nodules (e.g., Schmidt, 2009). Although data are few, the $\delta^{13}C$ and $\delta^{18}O$ values appear to be crudely correlated in lacustrine and paleosol carbonates. This suggests that the lake waters had a short 'residence time' and may have evolved somewhat from river inflow water. Consequently, these were not entirely hydrologically 'open' lakes. Similar relationships have been documented for modern lakes (Talbot and Kelts, 1990), Neogene–Quaternary lake deposits of Africa (Cerling and Hay, 1986; Cerling et al., 1988), and Oligocene lake deposits of Spain (Anadon and Utrilla, 1993). The isotopic composition of Javelina lacustrine carbonates is comparable, particularly to those of Olduvai lake deposits, except for lighter carbon isotopic composition, in keeping with an exclusively C3 Late Cretaceous vegetation. The $\delta^{18}O$ values are similar to those from the Olduvai lacustrine carbonates and suggest similar mean annual temperatures.

Finely disseminated particulate organic matter from floodplain paleosols, probably derived from leaves, twigs, and wood, yields $\delta^{13}C$ values ranging from −24.69‰ to −33.81‰ (mean = −28.7‰), consistent with the range reported for modern C3 vegetation (Fig. 11; Table 2). In contrast, samples of organic matter from lacustrine mudstone yield a narrow range of $\delta^{13}C$ values, averaging −23.14‰ and outside the range for soil organic matter (Fig. 11). Schmidt (2009) reported similar isotopic values for Javelina alluvial and lacustrine organic matter. This suggests that aquatic plants (freshwater macrophytes, algae, or mosses) were isotopically distinct from terrestrial plant material (forest litter). Comparable isotopic distinction is found in modern lakes and streams where organic productivity in aquatic environments is high and where the dissolved inorganic carbon fixed by aquatic plants differs from the atmospheric carbon dioxide ($CO_2$) used by land plants (e.g., Fry and Sherr, 1984). Osmond et al. (1981) found that aquatic plants in lakes or slowly flowing water had $\delta^{13}C$ values enriched relative to those growing in rapidly flowing waters, because of uptake in unstirred water of dissolved bicarbonate ($HCO_3^-$) rather than $CO_2$ derived from respiration of decomposing C3 plant material.

The radial fibrous calcite concretions and coatings on bones from the channel-lake facies yield $\delta^{18}O$ values slightly more negative than primary lacustrine carbonates and $\delta^{13}C$ values dramatically depleted compared with the primary carbonates (e.g., Schmidt, 2009). Fabric relationships suggest that the radial-fibrous calcite is an early diagenetic precipitate. It is similar in appearance and isotopic composition to fibrous vein-filling calcite described by Anadon and Utrilla (1993) in Oligocene lacustrine deposits. In addition to fabric relationships, the isotopic values are consistent with precipitation of the calcite soon after burial, in association with bacterial sulfate reduction and oxidation of organic matter in the sediment. Such an origin is supported by the association of small pyrite crystals with this form of calcite. One sample of coarsely crystalline calcite spar cement from the late-stage void fill of a pterosaur bone yields a $\delta^{13}C$ value significantly enriched (−4.92‰ vs. PDB) relative to primary lacustrine calcite and early diagenetic fibrous calcite. This suggests that precipitation of late-stage calcite accompanied fermentation of organic matter and bacterial methanogenesis during deeper burial of the sediment (e.g., Schmidt, 2009).

## INVERTEBRATE FAUNA AND ICHNOFAUNA

Several taxa of aquatic gastropods are found in abandoned channel-lake and stream channel facies (Fig. 12). Three species are common. A small, high-spired pleurocerid (*Goniobasis* cf. *G. tenera*) occurs in fluvial and lacustrine facies as accumulations of well-preserved specimens. This species is typically 10–15 mm in length, with a body whorl 5–7 mm in diameter. There are axial plications on the apical whorls, and all whorls have five prominent raised spiral lirae. A small viviparid (*Viviparus* cf. *V. trochiformis*) occurs as isolated individuals, some found directly associated with pterosaur remains. These have a smooth trochiform shell with slightly curved growth lines and range from 10–25 mm in length. A third common species (*Viviparus* sp.) is very large and low-spired, with a body whorl up to 40 mm in diameter, and a similar length. These are preserved as accumulations of steinkerns, usually in floodplain facies. Fragments of replaced shell material adhering to some of the steinkerns suggest faint spiral ornamentation. Small physid gastropods (*Physa* sp.) and

Downloaded From: https://bioone.org/journals/Journal-of-Vertebrate-Paleontology on 24 Apr 2024
Terms of Use: https://bioone.org/terms-of-use

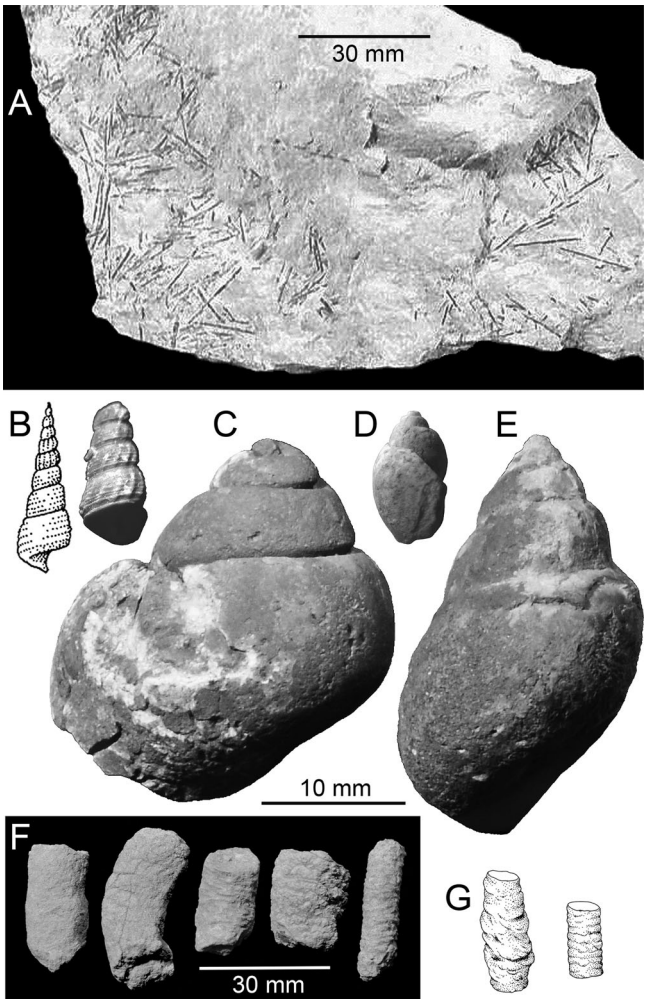


FIGURE 12. **A**, sediment matrix from the Amaral Site on 'Pterodactyl Ridge' showing carbonized palm vascular tissue on bedding planes. **B**–**F**, typical gastropods and ichnofossils of the Javelina Formation including **B**, *Goniobasis* cf. *G. tenera* with drawing of composite specimen, **C**, *Viviparus* sp., **D**, *Physa* sp., **E**, *Viviparus* cf. *trochiformis*, and **F**, example segments of burrow casts showing variation in wall sculpture from smooth (left) to verrucose (right). **G**, drawings of probable arthropod dwelling burrow casts showing those with irregularly sculptured walls (left) and verrucose pelleted wall structure (right).

small, thin-shelled unionid bivalves occur less frequently in lacustrine facies (Fig. 12).

The abandoned channel-lake facies is extensively bioturbated. Three common burrow types are present in these sediments (Figs. 12, 13). Two appear to represent dwelling burrows (domichnia) and the other a feeding trace (fodinichnia). The most common dwelling structure is a vertical to subvertical, straight or gently curved, smooth-walled burrow ranging from 1.0 to 2.5 cm in diameter and 10–50 cm in length. Because the burrow filling and the host sediment are similarly colored, these burrows are difficult to see in an unweathered condition. They are circular in cross-section and rarely branch. Such burrows are present throughout the coarsening-upward cycles in the lacustrine facies but are concentrated in the interbedded siltstone and very fine sandstone beds in the upper part of each cycle. Several cross-cutting generations of these burrows are distributed several centimeters apart within each bed. Most burrows terminate in blunt, rounded bottoms, but some end in short horizontal gallery systems. At one locality (TMM 42489), many of the burrows terminate in radial, star-shaped galleries (Fig. 13). The burrows are typically filled passively with sediment slightly finer grained than the surrounding matrix. Nevertheless, many burrows were filled actively (at least in part) with pelleted micrite, and these show a crude meniscate structure. Such burrows are present in the sediment surrounding the bone-bearing levels and within the sediment fill of some of the larger bones. These burrows are most similar to the 'type 6' and 'type 8' domichnia of Bown and Kraus (1983), who attributed them to insects, molluscs, or decapod crustaceans. Beds that are pervaded with this sort of burrow also have short, randomly oriented horizontal feeding traces and fecal castings on their upper surfaces.

A second common burrow type has a distinct, irregularly sculptured wall structure (Figs. 12, 13). These burrows range from 1.0 to 1.5 cm in diameter and from 10 to 30 cm in length. They are vertical to gently curved, with a circular cross-section. These burrows occur in the same beds as the more common smooth-walled burrows, and except for their wall structure they are otherwise similar. These burrows are smaller (both in length and diameter) than the 'type 9' domichnia of Bown and Kraus (1983) but are similar in form and verrucose wall surface. They may be the work of decapod crustaceans.

The third common burrow type consists of horizontal to subhorizontal, straight, simple-branching tubes with a diameter of 5–10 mm (Fig. 13). No striations or other wall structures are apparent, nor do enlarged terminations exist. These burrows tend to be more abundant in the finer-grained mudstone beds separating siltstone layers, where the vertical burrows are concentrated. Oriented clay linings are present around the walls of several examples studied in thin section. This burrow type is similar to the 'type 5' fodinichnia of Bown and Kraus (1983), who interpreted them as foraging galleries of either insects or oligochaetes.

The extensive bioturbation in the lacustrine facies indicates that the lake water was well oxygenated and supported a diverse soft-bodied macroinvertebrate infauna. Several levels of bioturbation within each coarsening-upward lacustrine sequence indicate that this facies accumulated episodically. Colonization of the sediment must have occurred during quiescent periods between sedimentation events.

## FLORA

Large logs, generally 40–60 cm in diameter, but ranging up to 80 cm, are relatively common in Javelina stream channel facies (Fig. 6). Stumps rooted in overbank floodplain facies are observed in at least two localities. The most common variety is the large dicotyledonous angiosperm *Javelinoxylon multiporosum* (Wheeler et al., 1994). This tree has affinities with the modern order Malvales, which includes predominantly tropical and subtropical families. Vernacular names for some modern malvaleans include the kapok, baobab, and balsa (Bombacaceae); linden and basswood (Tiliaceae); mallow (Malvalaceae); or cola nut and cocoa trees (Sterculiaceae). The largest *Javelinoxylon* trunks were from trees with a straight, slightly buttressed trunk lacking low branch points and with estimated crown heights of at least 30 m (Wheeler et al., 1994). The absence of distinct growth rings in *Javelinoxylon* and other features of the wood anatomy are consistent with a warm, dry, nonseasonal climate and a tropical lowland environment for the Javelina Formation (Wheeler et al., 1994). Moreover, given the form of its trunk, and great estimated crown height, *Javelinoxylon* was probably not an early successional 'pioneer' species, but a canopy tree of the mature forest. Several other dicot woods occur rarely, all marked by unusually high amounts of parenchyma (Wheeler and Lehman, 2000).

Downloaded From: https://bioone.org/journals/Journal-of-Vertebrate-Paleontology on 24 Apr 2024
Terms of Use: https://bioone.org/terms-of-use

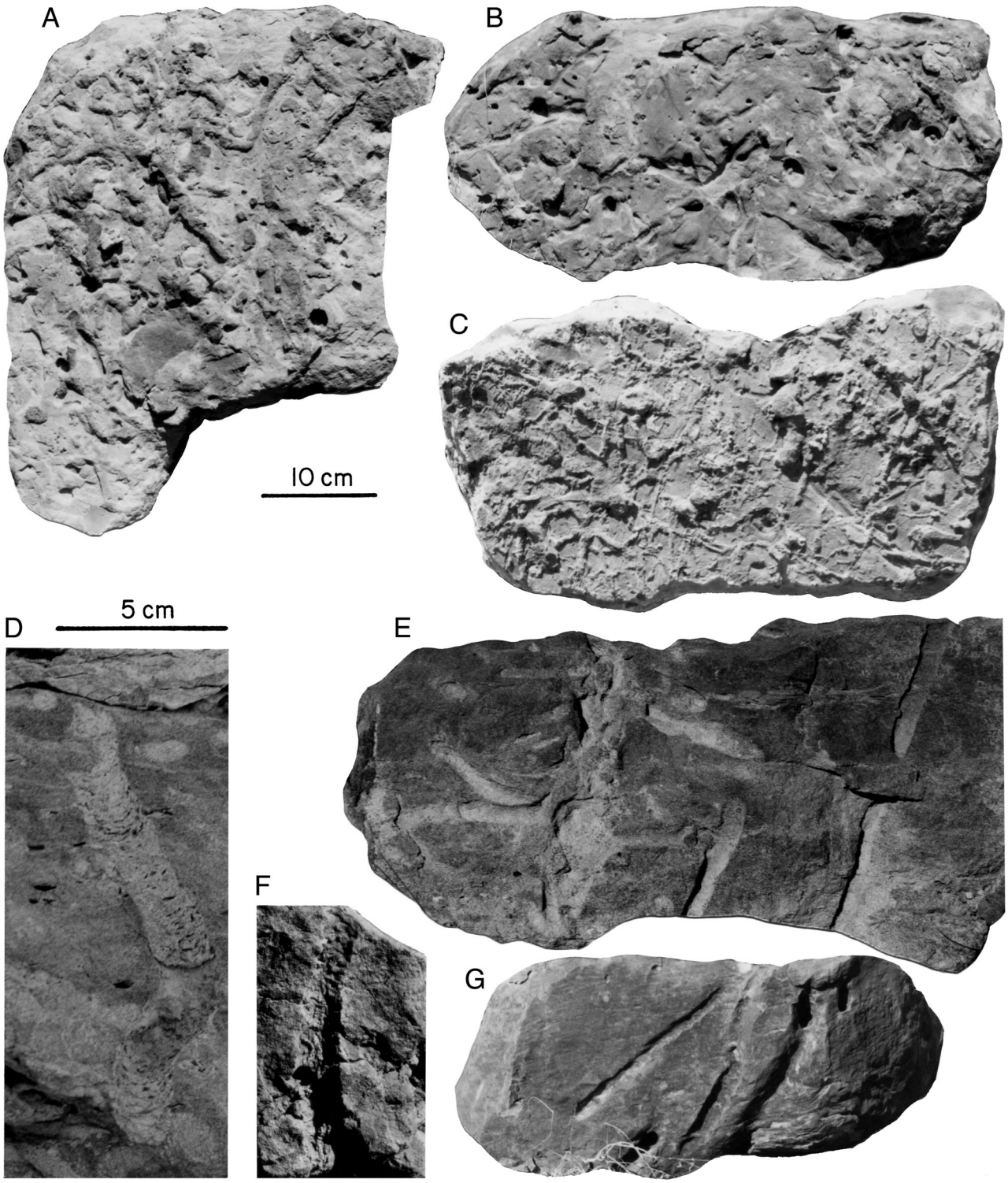


FIGURE 13. **A**–**C**, examples of typical ichnofossils found in channel-lake and stream channel facies of the Javelina Formation. **A**, lower bedding plane surface of thin sandstone bed in channel-lake facies showing predominantly horizontal burrows; **B**, upper bedding plane of same sandstone bed showing entrances to predominantly vertical burrows; **C**, lower bedding plane surface of thin sandstone bed in channel-lake facies showing horizontal traces radiating from bases of vertical burrows. **D**–**G**, cross-sections of thick sandstone beds in upper stream channel facies showing **D**, burrows with meniscate structure filled with micrite pellets, **E**, radiating horizontal gallery systems, **F**, burrows with verrucose pelleted wall structure, and **G**, simple unbranched subvertical smooth-walled burrows. The 10-cm scale bar applies to **A**–**C**, **E**, and **G**, and the 5-cm scale bar applies to **D** and **F**.

Many specimens of *Javelinoxylon* wood are infested with fossil termite galleries (Rohr et al., 1986). The termite borings and fecal pellets are consistent with the work of modern 'dry wood' termites, the majority of which are found today in tropical and subtropical regions. Fragmentary logs of an araucariacean conifer are also present in the Javelina Formation (Wheeler and

Downloaded From: https://bioone.org/journals/Journal-of-Vertebrate-Paleontology on 24 Apr 2024
Terms of Use: https://bioone.org/terms-of-use

Lehman, 2005). Modern Araucariaceae are found in South America, Southeast Asia, Australia, and Pacific islands (e.g., monkey puzzle tree, candelabra tree, Norfolk Island pine).

Wood is rarely found in the abandoned channel-lake facies. Instead, slender axes of an unidentified aquatic vine occur sporadically (a wood type described informally as the 'Javelina Vine' by Wheeler and Lehman, 2000). Bedding planes in channel-lake facies are typically covered with reworked macerated fragments of palm vascular tissue (Fig. 12A). In particular, pterosaur bones from the main quarry level on Pterodactyl Ridge are associated with a bedding plane covered with small, carbonized fragments of palm fibers. Larger fragments of palm wood and impressions of palm fronds are relatively common in abandoned channel-lake and stream channel facies. The stalks and leaves are similar to modern palmetto palm (*Sabal*) found in Central America, the Caribbean, Mexico, and southern U.S.A. (Manchester et al., 2010).

## TAPHONOMY OF *QUETZALCOATLUS* SITES

Studies of pterosaurian taphonomy during the past 45 years include the spectacular occurrences in the marine Solnhofen and Niobrara deposits (Wellnhofer, 1970), lacustrine burials in Kazakhstan, Jurassic and Cretaceous sites in the former Soviet Union and Mongolia (Bakhurina and Unwin, 1995; Unwin and Bakhurina, 2000), and the Santana and Crato lagoonal sediments of northeastern Brazil (Beurden, 1971; Frey and Martill, 1994; Kellner, 1994). Reworked deposits have been noted by Buffetaut (1995; Cambridge greensands) and Bell and Padian (1995; a Cretaceous flood event in northern Chile). The taphonomy of fragmentary Upper Cretaceous azhdarchid pterosaurs from fluvial deposits in the Kyzylkum Desert in Uzbekistan has been discussed at length by Nesov (1991c), Archibald et al. (1998), and Unwin and Bakhurina (2000).

The pterosaur occurrences in Big Bend furnish taphonomic data from a somewhat different context than those previously reported. *Quetzalcoatlus* specimens have been found in all three facies of the Javelina Formation (Figs. 5, 6). The type specimen of the gigantic *Quetzalcoatlus northropi* (TMM 41450-3, an incomplete wing) is from the base of a stream channel deposit, and several additional specimens from Pterodactyl Ridge (e.g., TMM 42889-1, an isolated cervical vertebra) have also been recovered from basal lag deposits of stream channel facies. A few specimens (e.g., TMM 41839-2 to TMM 41839-12, fragmentary metatarsals and phalanges) were found in overbank floodplain facies. However, the great majority of pterosaur specimens from Big Bend were recovered from the abandoned channel-lake facies. A few of these specimens are partly articulated or are associated remains of single individuals (e.g., TMM 42489-1, an incomplete skull and jaws with associated articulated neck; TMM 41961-1, a skeleton including skull and jaws of *Quetzalcoatlus lawsoni*, sp. nov.; Andres and Langston, 2021). These individual burials are of special interest because some articulation or close association is retained, and they include fragmentary skulls and jaws (Kellner and Langston, 1996; Andres and Langston, 2021). Moreover, a few fragments of fossil eggshell identified as ornithoid-ratite type, not necessarily produced by pterosaurs, were discovered in the matrix adjacent to TMM 41961-1.

The major source of pterosaur remains on Pterodactyl Ridge is a monotaxic bone bed ('Konzentrat-Lagerstätte' of Seilacher, 1970) in the abandoned channel-lake facies containing only bones of *Quetzalcoatlus lawsoni*, sp. nov. (Andres and Langston, 2021). This prolific fossiliferous zone (the 'main quarry level' of Figs. 5, 6, 8) is referred to here as the 'Amaral Site' in recognition of Mr. William Amaral, who discovered the first pterosaur bones at this site in 1973. Bones at the Amaral Site occur as disarticulated scattered elements and in concentrated associations of elements within a single stratigraphic interval not more than 1 m in thickness. Some 270 identifiable bones attributable to *Quetzalcoatlus lawsoni*, sp. nov., have been recovered from the Amaral Site which is exposed on the deeply dissected southerly dip slope of Pterodactyl Ridge (Figs. 3, 4). Age classes are not evident in the bones, which display a size difference of only about 10% between the largest and the smallest individuals. Their occurrence within a narrow stratal zone and the absence of differential weathering clearly indicate a brief nonattritional accumulation (Behrensmeyer, 1991).

Wann Langston's field parties visited the Amaral Site repeatedly over a span of 23 years. Complete field records were kept during all phases of collecting; all identifiable bones were collected and their positions recorded (Andres and Langston, 2021; Brown et al., 2021). Observations of sedimentary structures were hampered by the monochromy of the rocks and the homogeneity of the fine-grained matrix. Tabular jointing in the beds often deviates but slightly from the bedding, thus complicating measurement of attitudes in the strata and tracing of the fossiliferous horizon from site to site and even within a single quarry. Thus, determination of the sedimentary and stratigraphic relationships between bones and their context is less precise than could be wished for.

### Minimum Number of Individuals

The main fossiliferous horizon at the Amaral Site now comprises an area of about 138 $m^2$. The observed spatial density of bones on the outcrop is 1.7 bones/$m^2$, but this value includes four local bone concentrations (WL-A, WL-B, WL-C, and WL-D; see Brown et al., 2021) where the density is greater than elsewhere. Thus, large areas of the bone-bearing horizon are nonfossiliferous. Such patchiness renders suspect estimates of total numbers of bones and hence of individuals represented within arbitrarily defined areas. For sampling purposes, an originally intact, roughly trapezoidal area of 2,429 $m^2$ is assumed, delimited by bones at the periphery of the outcrop and enclosing not only the fossil sites but also the intervening area now lost to erosion or still covered by overburden.

Of the 270 identifiable bones collected in the four local concentrations, complete bones number 132. Limited duplication of elements occurs within each concentration, showing that these assemblages are composite. Because all bones in the entire assemblage represent individuals of roughly comparable size—ratios of the longest to the shortest examples among major limb bones vary from 1.05 (ulna) to 1.15 (wing phalanx IV-I)—it is impossible to assign with assurance most of the single bones within a concentration to a particular individual.

Estimating the number of individuals present in bone-bed assemblages is usually imprecise owing to a host of biases in sampling, unknowns, and necessary but possibly inaccurate assumptions (Martin, 1999). Attempts to determine the minimum number of individuals (MNI) at the Amaral Site are no exception. After applying various techniques summarized by Klein and Cruz-Uribe (1984), Badgley (1986), and Lyman (1994), the simple procedure of counting the number of frequently occurring elements in the Amaral Site matching them for size, and sorting left and right sides was adopted. This method yields conservative results, tending to underestimate the actual number of individuals (Gilinsky and Bennington, 1994).

Of paired bones, the most frequently occurring elements are humeri (N = 13). Because of their geographic proximity and size, the four humeri associated with TMM 42422 and TMM 42180 are regarded as right and left members, respectively, of these two associated skeletons. Less confidently, TMM 41954-26 and 41954-27, right and left humeri, respectively, are assigned to a single individual. Filtering the seven remaining humeri for size and possible pairs suggests that each bone may represent

Downloaded From: https://bioone.org/journals/Journal-of-Vertebrate-Paleontology on 24 Apr 2024
Terms of Use: https://bioone.org/terms-of-use

TABLE 3. Census of *Quetzalcoatlus lawsoni*, sp. nov., identifiable bones preserved at the Amaral Site number of bones expected, and percentage recovered for each element (assuming MNI = 15).

| Element | No. found | No. expected | % Represented |
|---|---|---|---|
| Cranium | 7 | 15 | 47 |
| Mandible | 5 | 15 | 33 |
| Atlas-axis | 2 | 15 | 13 |
| Cervical 3 | 9 | 15 | 60 |
| Cervical 4 | 1 | 15 | 7 |
| Cervical 5 | 15 | 15 | 100 |
| Cervical 6 | 10 | 15 | 67 |
| Cervical 7 | 8 | 15 | 53 |
| Cervical 8 | 2 | 15 | 13 |
| Cervical 9 | 2 | 15 | 13 |
| Cervical indeterminate | 4 | | |
| Free dorsal ribs[a] | 3 | 240 | 1 |
| Notarium | 3 | 15 | 20 |
| Free dorsal vertebrae[b] | 0 | 45 | 0 |
| Sacrum | 1 | 15 | 7 |
| Pelvis | 2 | 15 | 13 |
| Caudal vertebrae[c] | 0 | 180 | 0 |
| Sternum | 4 | 15 | 27 |
| Scapulocoracoid | 8 | 30 | 27 |
| Humerus | 12 | 30 | 40 |
| Ulna | 10 | 30 | 33 |
| Radius | 8 | 30 | 27 |
| Pteroid | 3 | 30 | 10 |
| Proximal syncarpal | 7 | 30 | 23 |
| Distal syncarpal | 10 | 30 | 33 |
| Distal lateral carpal | 3 | 30 | 10 |
| MC IV | 15 | 30 | 50 |
| Ph IV-1 | 13 | 30 | 43 |
| Ph IV-2 | 13 | 30 | 43 |
| Ph IV-3 | 9 | 30 | 30 |
| Ph IV-4 | 5 | 30 | 17 |
| MCs I, II, III | 7 | 90 | 8 |
| Manual phalanges[d] | 15 | 180 | 8 |
| Manual claws | 9 | 90 | 10 |
| Femur | 9 | 30 | 30 |
| Tibia + fibula | 11 | 30 | 37 |
| Free tarsals[e] | 4 | 60 | 7 |
| MTs I–V | 13 | 150 | 9 |
| Pedal phalanges[f] | 2 | 300 | <1 |
| Pedal claws | 6 | 120 | 5 |
| Total | 270 | | |

[a]Assuming 8 for each side.
[b]Assuming 3 (6 in notarium and 11 total).
[c]Assuming 12 vertebrae in tail.
[d]Assuming 1 on digit I, 2 on II, and 3 on III.
[e]Assuming 2 total each pes.
[f]Assuming 1, 2, 3, 4, and 0 for digits I through V, respectively.

one individual, giving MNI = 10. Wing phalanx IV-I also predicts MNI = 8–10; however, an estimate based on the putative fifth cervical vertebrae yields MNI = 15. Because these are minimal values, MNI = 15 is accepted as the best estimate, but certainly a conservative one (Table 3).

In a more speculative realm are estimates of the numbers of individuals originally present at the Amaral Site. Based on the inferred density of bones (1.7 bones/$m^2$) in excavated rock, the total number of elements formerly present and/or still buried here would have been in the neighborhood of 4,100. Then, based on the MNI = 15 and an estimated number of likely-to-be recovered elements in the *Quetzalcoatlus* skeleton (≈138), the formerly intact area at the Amaral Site could have contained remains of 30 individuals. These actual and estimated numbers are consistent with the idea that some pterodactyl species were gregarious (Nesov, 1991c; Kellner, 1994; Bell and Padian, 1995).

## Bone Breakage

Many bones at the Amaral Site were damaged before burial. Apophyses and parts of centra are missing from vertebrae, a few humeri are represented only by their ends, and other wing bones lack one or both ends, or the shaft. Specimen TMM 41954 includes broken parts that remained in close proximity and, although shifted out of alignment, appear to have been held together by soft tissues until buried. More often, however, broken segments are isolated.

Of several patterns of breakage noted in robust long bones by Shipman (1981:fig. 5.2), the following have been recognized at the Amaral Site step or columnar fracture of the shaft (wing phalanx IV, metacarpal IV, radius), 'V'-shaped fracture of the shaft (humerus, ulna), sawtooth fracture (wing phalanx IV, femur), smooth perpendicular break through the shaft (humerus), irregular perpendicular break through the shaft (coracoid, humerus), and spiral fracture of the shaft (humerus, radius, ulna, tibia). Another kind of breakage involves longitudinal and diagonal fracture of the shaft (cervical vertebrae, unidentified long bones, metacarpal IV).

The broken bones found at the Amaral Site seem more consistent with dry bone breakage (Hill, 1980; Shipman, 1981) than with fresh bone fracturing (Johnson, 1985), although a few fractures suggest 'green twig' breakage. Given the wide dispersal of broken bone segments, the breakage may be attributable to trampling rather than to any postburial process. If trampling is responsible, it took place on a firm substrate because no bones display any inclination to the horizontal (Hill and Walker, 1972). Marking of the bone surfaces as sometimes attributed to trampling is not evident, and that tramplers were large may be ruled out by the absence of inclined bones. The spacing of fragments (up to the order of meters) could be partly or wholly due to animal disturbance prior to burial. Although the identity of the supposed trampler is unknown, tooth punctures in some bones (see below) may indicate the presence of crocodilians. No crocodilian bones have been found, however, at any of the pterosaur localities, and they are rare elsewhere in the Javelina Formation.

## Bone Weathering

The bones at the Amaral Site exhibit complicated cracking patterns of both biostratinomic and diagenetic origin (Fig. 14). There is little or no evidence of flaking or exfoliation of cortical laminae, and most elements can be assigned to weathering stage 2 of Behrensmeyer (1978). Many limb bones and long cervical vertebrae exhibit longitudinal and mosaic eggshell cracking, but such massive bones as carpals and the ends of humeri and scapulocoracoids are little broken. Longitudinal cracks typically penetrate the entire thickness of the cortex of otherwise intact bones. Such cracking is believed to be largely due to subaerial weathering (Behrensmeyer's weathering stage 1), and some of the curvilinear cracking in the pterosaur bones may be so attributed, especially where cracking is more extensive on the upper (exposed) surface than on the bottom (e.g., TMM 41954-55). Nevertheless, rectilinear cracking (e.g., TMM 42138-1) is present on all the surfaces of long bones, and the cracks are so numerous that had they all developed biostratinomically one would expect more or less complete disruption of the thin and hollow bones. Much of this rectilinear cracking likely resulted from displacive crystallization of microcrystalline calcite shortly after burial (see below). Because surface weathering did not progress much beyond weathering stage 1, bones may have been exposed for less than a year, probably much less. Surface texture is often exquisitely preserved, and there is no evidence of long distance transport (abraded ends or rounded fracture surfaces).

The bone-bearing zone lies within fine-grained sediment; it is not associated with a marked erosional surface nor with a layer of coarse detritus and so does not represent the product of a severe storm or flood event. Nevertheless, a preferred current orientation of long bones (cervical vertebrae, wing and limb

Downloaded From: https://bioone.org/journals/Journal-of-Vertebrate-Paleontology on 24 Apr 2024
Terms of Use: https://bioone.org/terms-of-use

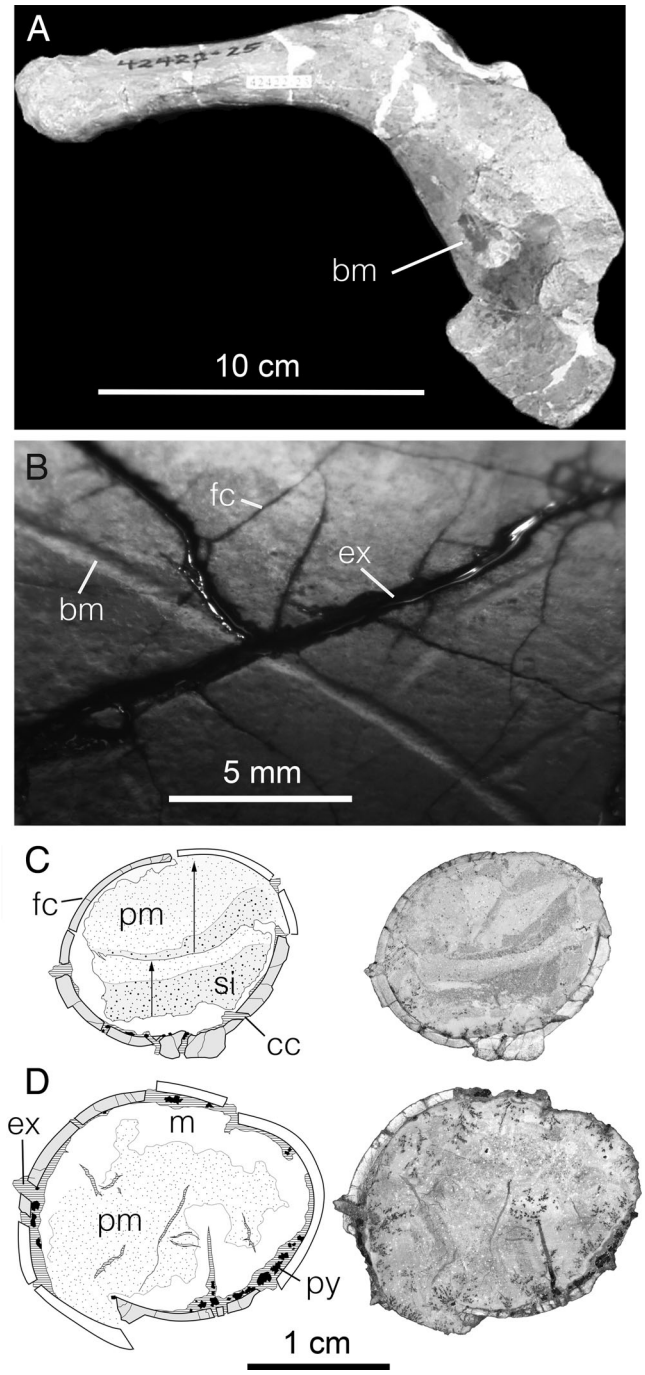


FIGURE 14. Taphonomic features of *Quetzalcoatlus lawsoni*, sp. nov., bones from the Amaral Site. **A**, conical bite mark in scapulocoracoid (TMM 42422-25). **B**, detail of cortical surface in fragmentary wing metacarpal (TMM 44037-1) showing cross-cutting relationships of bite marks followed by fine cracks due to weathering, and later expansion cracks due to displacive mineralization. **C**–**D**, camera lucida drawings of bone cross-sections (left) with corresponding photographs (right) showing **C**, bone with open broken end partially filled with detrital sediment (TMM 44037-1) and preserved in-the-round; **D**, bone filled entirely with chemical sediment (TMM 44037-2) and partially collapsed; sequential fill begins with microbial pustular micrite precipitated circumferentially; geopetal terrigenous and carbonate silt deposited in lower part of medullary cavity, followed by pelloidal micrite in fining-upward successions (indicated with arrows) and coarsely crystalline calcite spar with pyrite crystals in expansion cracks and where internal fill has pulled away from bone surface. **Abbreviations**: **bm**, bite marks; **cc**, coarsely crystalline calcite spar; **ex**, expansion cracks; **fc**, fine cracks; **m**, microbial pustular micrite; **pm**, pelloidal micrite; **py**, pyrite crystals; **si**, geopetal terrigenous and carbonate silt.

elements) is apparent throughout the Amaral Site with one modal orientation parallel to the local southeastwardly paleostream flow direction and another mode normal to this (Fig. 10). Bimodal orientation is common in hydraulically transported long bones under very shallow, partially emergent conditions (Voorhies, 1969; Shipman, 1981). Current energy was sufficient to have removed ribs (only one example collected) and free thoracic vertebrae (none found) and to shift other parts away from such complex (easily anchored) segments as a pelvis and two notaria, elements that are underrepresented in the sample, assuming that such 'meaty' portions were not carried away or destroyed by predators or scavengers.

## Scavenging

Limited evidence of possible scavenging (or predation) is seen on several bones from the Amaral Site. The most convincing example is a conical depressed 'trap door' puncture 9 mm in diameter near the distal end of a fourth metacarpal (TMM 42138-1), and another example is a similar puncture on the medial surface near the proximal end of a left coracoid (Fig. 14; TMM 42422-25). Two additional round holes are present in the latter bone, lying in the closed scapulocoracoid suture within the glenoid fossa, and what may be an answering puncture lies opposite these on the medial surface. The presumed mate to this scapulocoracoid (TMM 42422-12) displays similar damage. Two vertebrae (TMM 41544-4 and TMM 42180-2) also appear to have similar damage, and a presumed fourth cervical vertebra (TMM 41544-8) may exhibit another example of a (13 mm wide) puncture. A sternum (TMM 42180-12) contains a straight furrow, 7 mm wide, which passes upward along the right side a short distance posterior to the coracoid facets and ends dorsally in a blunt, rounded depression. The right quadrate bone of TMM 42422-30 contains three 'perforations' that may have resulted from a bite (Kellner and Langston, 1996). Finally, a mandible (TMM 42161-2) contains two 15-mm-wide holes, one dorsal and the other ventral, lying across the sagittal plane some 75 mm anterior to the end of the symphysis. Edges are cleanly broken, but there is no evidence of depressed fragments within. The openings are not directly opposite one another; the center of the lower one lies 6 mm behind that of the upper one. Interestingly, no shed teeth or other remains of likely predatory or scavenging animals have been found at the Amaral Site.

Because their sizes are similar, the circular perforations were initially attributed to burrowing infauna, but the 'trap door' fractures and offset openings in the mandible and coracoid argue against this interpretation. Such features accord better with the shape (blunt and conical) and arrangement (serial alternation of upper and lower dentition) of the teeth in crocodilians. Another, but less likely, source of the damage is 'pecking' by living pterosaurs. The prevalent circular shape of the penetrations seems inconsistent with the chisel-shaped cross-section of the tip of the mandible or an inferred triangular section of the cranial rostrum. On the other hand, termites and beetle larvae may chew bones, leaving rounded borings (e.g., Shipman, 1981), so some of the circular perforations may have resulted from nonvertebrate scavenging. Not surprisingly, there is no evidence of vertebrate chewing or gnawing.

## Bone Transport

Pterosaur carcasses may have responded to traction transport hydrologically more like birds (e.g., Bickart, 1984) than like other vertebrates, not only because they have similarly hollow and light weight bones but also because the flight membranes would easily have become anchored by sediment accumulation. In one instance (TMM 42180-14; Fig. 15), a wing skeleton is

Downloaded From: https://bioone.org/journals/Journal-of-Vertebrate-Paleontology on 24 Apr 2024
Terms of Use: https://bioone.org/terms-of-use

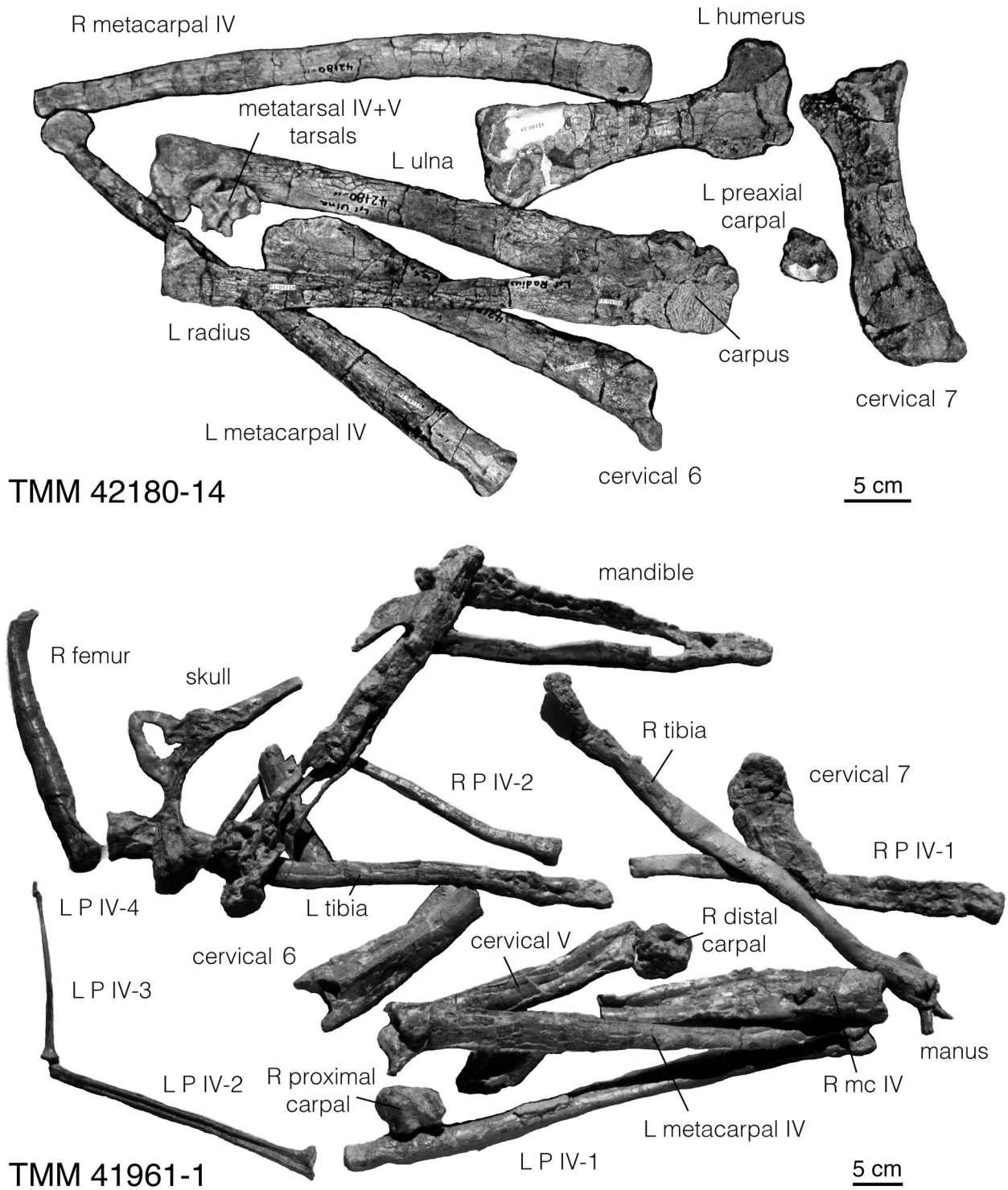


FIGURE 15. TMM 42180-14 (above) and TMM 41961-1 (below), two associated skeletons of *Quetzalcoatlus lawsoni*, sp. nov., showing the relative positions of elements as preserved. Some elements associated with TMM 41961-1, e.g., fragments of left ulna and left femur, were collected as surface 'float' and their positions relative to those shown cannot be accurately determined.

folded upon itself and may have acted as an obstruction to the movement of other parts of the skeleton. In another instance (TMM 41961-1; Fig. 15), the wing metacarpal and its associated phalanges are tightly flexed at the metacarpophalangeal joint but the phalanges are extended. Both of these circumstances might be attributed to anchoring of the wing membranes by sediment accumulation.

A generalized skeletal disarticulation and disintegration sequence, like those formulated for mammals (e.g., Hill, 1980), has not yet been defined for pterosaurs, although their carcasses

Downloaded From: https://bioone.org/journals/Journal-of-Vertebrate-Paleontology on 24 Apr 2024
Terms of Use: https://bioone.org/terms-of-use

may have disarticulated in a manner similar to that observed for birds (Schäfer, 1962; Weigelt, 1989). A few stages in the taphonomic sequence can be inferred on the basis of observations of Solnhofen and Santana specimens (e.g., Wellnhofer, 1970; Kellner, 1994). For example, the thoracic cavity presumably collapsed shortly after death and wings separated from the shoulder girdle at an early stage of degradation. Wings, hind limbs, and necks tended to remain intact longer, and approximately in that order, depending on the degree of desiccation and speed of decay and burial. Burials in quiet, anoxic environments (e.g., Solnhofen; Karatau Ridge in Kazakhstan) tend to remain relatively intact; heads tend to remain attached to the neck, and tails tend to remain articulated. At the Amaral Site, the carcasses were almost completely disarticulated before burial. The absence or rarity of small, light, or fragile skeletal elements such as ribs, notaria, free thoracic vertebrae, and pelves compared with the relative abundance of larger, dense, compact elements such as humeri, posterior cervical vertebrae, and proximal wing phalanges suggests that the Amaral Site preserves a residual 'lag' assemblage of elements most resistant to transport by current action. Three skeletal element representation groups may be discerned, based on the number of elements recovered versus those expected for an estimated MNI = 15 (Fig. 16; Table 3). The free thoracic and caudal vertebrae, sacra, ribs, smaller manual and pedal phalanges, and claws were recovered in numbers less than a quarter of those expected (Fig. 16, group 1). In contrast, more than half of the expected number of larger cervical vertebrae, fourth metacarpals, and humeri were recovered (Fig. 16, group 3). This accords with the interpretation of the latter as 'lag' elements and with the common occurrence of these bones as single isolated elements at other sites in the Javelina Formation as well as elsewhere in North America (e.g., Henderson and Peterson, 2006).

The inferred nonattritional character of the *Quetzalcoatlus lawsoni*, sp. nov., bone bed at the Amaral Site, the absence of similar concentrations elsewhere in the vicinity, an absence of age classes within the sample, and the apparent adult condition of the animals suggest that the remains are from a transitory flock of pterosaurs. One may speculate that this was part of a flock that settled here only to fall victim of unknown causes over a brief span of time, perhaps as little as a few days, given their preservation on a single stratigraphic horizon and similar state of bone weathering. The corpses were scavenged, possibly by crocodilians, although they were not very thorough in consuming the carcasses. The remaining skeletons were almost completely disarticulated, and many bones were broken. A brief period of subaerial exposure followed. The nearly unimodal arrangement of long bones, including cervical vertebrae, within each bone concentration at the Amaral Site suggests that each such concentration may represent one or a few individual burials, and if so, little transportation occurred. Transportation appears to have produced only modest shifting of the elements remaining in each skeleton, and they were buried rapidly.

### Diagenesis

The silty calcareous mudstone in which the bones are buried exhibits irregular lamination and soft-sediment brecciation features, indicating that this is primary sediment, not a result of later diagenetic precipitation. This and the interbedded siltstone layers contain abundant biogenic calcite and tiny carbonate spherules, probably of algal or microbial origin; and as noted, some associated burrows are filled with pelleted micrite. Vacuities in the medullar spaces of the bones are lined or filled with similar micritic lime sediment, also exhibiting lamination, brecciation, and clotted pustular fabric, suggesting a bacterial role in carbonate precipitation. Many bones exhibit a geopetal internal sediment stratigraphy (Figs. 14, 17). Initially, the bones were partially or completely filled with silty detrital lime sediment. Those bones that were filled completely at this stage are preserved in-the-round without much later crushing. Remaining voids then acquired a coating of clean laminated microcrystalline calcite, microbially precipitated and devoid of detrital silt. This coating is thickest in the lower parts of the internal void fillings. In most cases, the exterior surfaces of the bones are coated partially with lumpy masses of the same material, which also forms nodules and discontinuous layers around the bones. This coating must have initially been soft and leathery, because it is wrinkled, folded, and pulled away from the bone surfaces in places. As noted, the micritic sediment and coatings likely precipitated in shallow alkaline lake water (see above). Burrowing fauna pelletized the micritic sediment that partially fills the burrows.

Later, the lime sediment was cracked and brecciated while still soft. This probably took place during desiccation and/or compaction of the surrounding sediment. At this time, bones that had not been completely filled with sediment were further cracked and collapsed. Cracks in the bones and sediment matrix were next filled with radial fibrous calcite, and thick crusts of bushy radial fibrous calcite coated the exterior surfaces of the bones, filled large cracks, and formed separate nonossiferous nodules (Fig. 17). Radial fibrous calcite also forms an isopachous coating aggrading toward the center of larger remaining pores within the bones. This type of calcite contains little detrital silt, except between bundles of fibers. Although formed after the bones were buried, it must have precipitated very early in diagenesis (before lithification of the sediment) because it fills contorted soft-sediment cracks. Fragments and nodules of calcite with this radial fibrous structure are also reworked in adjacent stream channel deposits. Small spherules and aggregates of pyrite crystals are enclosed within the radial fibrous calcite. Hence, as noted (see above), the radial fibrous calcite probably precipitated under anaerobic conditions accompanying decay of organic matter in the sediment, in a shallowly buried reducing environment. After further compaction of the sediment, scalenodehral calcite and coarse blocky calcite spar filled the remaining pores and cracks (Fig. 17).

## DISCUSSION AND INFERENCE

The abandoned channel-lake facies is the least common of the sedimentary facies represented in the Javelina Formation. The repeated association and abundance of pterosaurs at several stratigraphic levels within this facies suggests that it represents an environment frequented by pterosaurs either throughout the year or during migration or nesting. The nonattritional death assemblage with a single size/age class represented at the Amaral Site suggests that *Quetzalcoatlus lawsoni*, sp. nov. (Andres and Langston, 2021), was at least occasionally gregarious and gathered in flocks of adult individuals. If the eggshell fragments found at several levels are attributable to *Quetzalcoatlus lawsoni*, it could indicate that these environments were nesting sites.

Extensive bioturbation throughout the channel-lake facies indicates that it supported an abundant soft-bodied macroinvertebrate fauna, probably crustaceans, insects, and annelids. A diverse freshwater gastropod and bivalve fauna was also present intermittently. As Langston (1981) suggested, this invertebrate fauna may have been the primary food resource for *Quetzalcoatlus lawsoni*. The absence in this facies of a typical aquatic vertebrate fauna, such as the fishes, turtles, and crocodilians found elsewhere in the Javelina Formation, implies that this aquatic environment was inhospitable in some way compared with normal stream channel environments. Abundant microbial precipitation of carbonate in the lakes may indicate that the waters were usually too alkaline to support a normal freshwater aquatic vertebrate fauna. Some present-day

Downloaded From: https://bioone.org/journals/Journal-of-Vertebrate-Paleontology on 24 Apr 2024
Terms of Use: https://bioone.org/terms-of-use

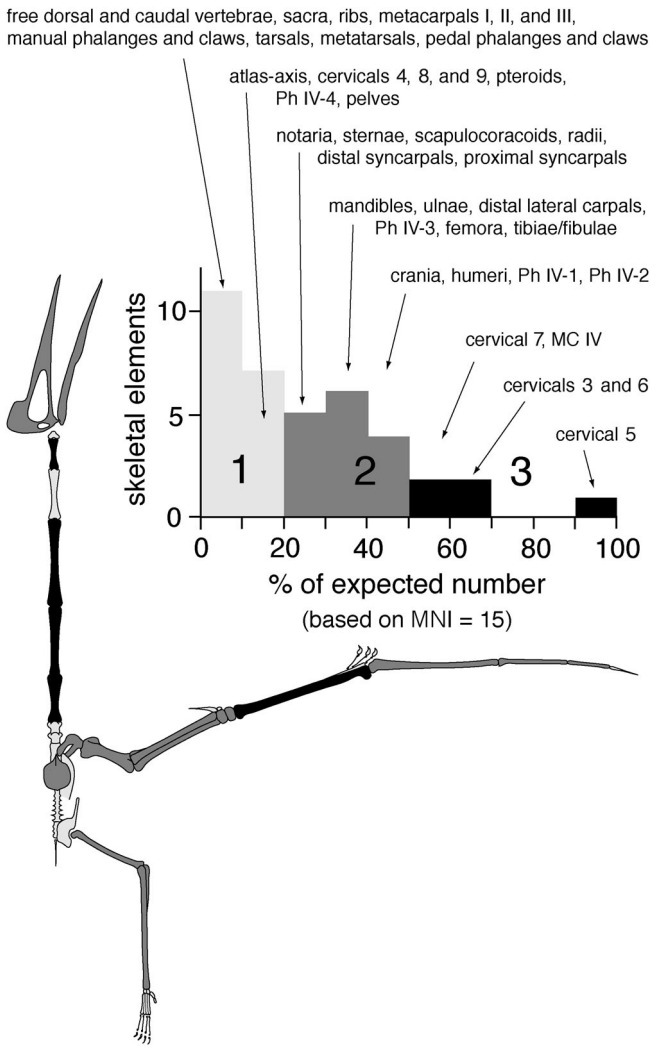


FIGURE 16. Relative abundance of *Quetzalcoatlus lawsoni*, sp. nov., skeletal elements preserved on the main quarry level at the Amaral Site (Table 3). The minimum number of individuals (MNI) is 15 based on cervical 5. Three skeletal element representation groups are shown on the histogram above and on the diagrammatic restoration, with elements most abundantly represented (>40%: black), those found in moderate abundance (20–40%: dark gray), and those very underrepresented (<20%: light gray).

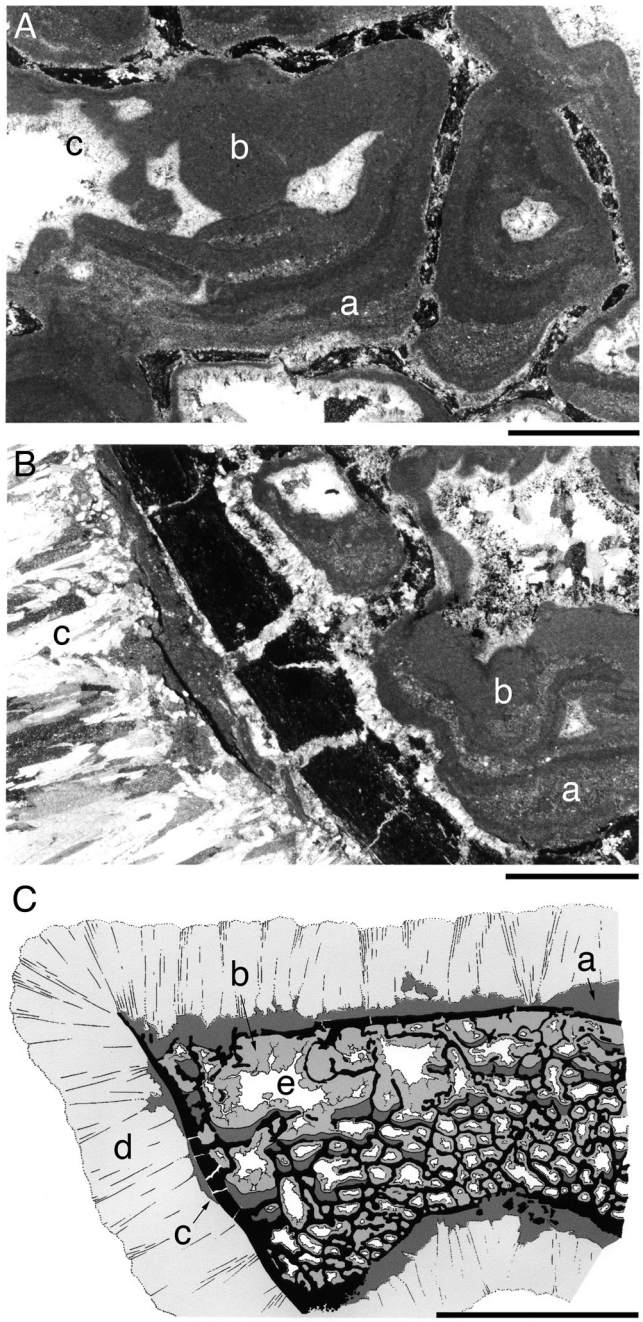


FIGURE 17. Photomicrographs and camera lucida drawing showing cross-section of *Quetzalcoatlus lawsoni*, sp. nov., bone (TMM 41954-1a) preserved in channel-lake facies at the Amaral Site, with typical sequence of in-filling and diagenetic features. **A**, photomicrographs (cross-polarized light) showing detailed filling of trabecular tissue (central part of bone shown in C); **B**, adjacent to cortical tissue (lower left of bone shown in **C**); **C**, camera lucida drawing of entire cross-section. Bone is surrounded and lower parts of vacuities are partly filled with multiple cycles of **a**, detrital silt and pelloidal micrite; remaining voids subsequently lined with **b**, clotted pustular micrite; **c**, late-stage cracks in cortical bone, voids; and **d**, exterior of bone are coated with radial-fibrous calcite; and remaining voids are filled with **e**, blocky equant calcite spar. Scale bars equal 1 mm (**A**, **B**) and 10 mm (**C**).

wading birds (e.g., flamingos, herons, cranes) inhabit alkaline lake environments, at least occasionally, and have a body plan generally similar to that of *Quetzalcoatlus lawsoni*. Cranes and storks are also among the largest of living birds, and many subsist in part on a diet of aquatic invertebrates similar to that hypothesized for *Quetzalcoatlus lawsoni* (e.g., whooping crane; Johnsgard, 1983).

Preservation of palm vascular tissue as primary organic detritus in the lacustrine deposits, as well as preservation of palm wood and frond impressions, suggests that areas immediately surrounding the lakes were vegetated with palmetto palms. Trunks of large dicot trees (*Javelinoxylon*), araucariacean conifers, and woody vine fragments in stream channel and floodplain facies indicate that the regional environment was an evergreen or semideciduous tropical forest. Absence of low branch points and estimates of crown height for *Javelinoxylon* indicate a continuous closed forest canopy over 30 m in height. *Quetzalcoatlus lawsoni* therefore appears to have been capable of aerial maneuvering in a densely forested landscape and must also have been capable of landing and takeoff from

Downloaded From: https://bioone.org/journals/Journal-of-Vertebrate-Paleontology on 24 Apr 2024
Terms of Use: https://bioone.org/terms-of-use

the ground in limited open spaces that surrounded channel-lake habitats. There were no nearby areas with marked topographic relief that would have allowed assisted takeoff from a high perch. Although height estimates suggest that isolated or emergent trees might have afforded such opportunities, the form of the pes in *Quetzalcoatlus lawsoni* appears poorly suited for perching on branches.

The 'giant' *Quetzalcoatlus northropi* is, in contrast, thus far known from only four or five specimens, all from fluvial channel facies, not lacustrine deposits, and not associated with remains of *Quetzalcoatlus lawsoni* (Table 1). This may indicate that *Q. northropi* favored a riparian habitat and led a more solitary lifestyle, although given so few specimens this is certainly speculative. Its presence in the Javelina Formation, although not in contemporaneous strata with fluvial facies elsewhere in North America (e.g., Hell Creek Formation), argues that there were some attributes of Javelina riparian environments better suited than elsewhere. If the two species of *Quetzalcoatlus* were truly contemporaneous, they may have been separated by slight habitat and behavioral differences, as are found in sympatric species of large wading birds today, for example in gregarious sandhill cranes and solitary blue heron that inhabit the same region of North America (e.g., Johnsgard, 1983).

The abundant remains of *Quetzalcoatlus lawsoni* and other azhdarchids throughout the upper part of the Javelina Formation suggest that the environments represented here were their preferred habitat. Although *Quetzalcoatlus lawsoni* or a similar azhdarchid is found in contemporaneous strata elsewhere in North America, for the most part these other occurrences are based on isolated single bones. Comparable fluvial and lacustrine facies are found throughout contemporaneous strata in the western interior of North America, and so the presence of riparian and lacustrine environments alone may not have been what attracted azhdarchid pterosaurs to the Big Bend region. Instead, the relatively low paleolatitude of Big Bend during Maastrichtian time (about 32°N), and high mean annual temperature (ca. 20°C), may indicate that azhdarchids favored tropical to subtropical climate. Paleotemperature proxy data show that the Late Cretaceous latitudinal temperature gradient was quite low, but even so it was sufficient to induce latitudinal biotic zonation (e.g., Lehman and Barnes, 2010).

The presence of well-developed calcic horizons in Javelina floodplain paleosols and their isotopic composition indicate a very warm (16–22°C mean annual temperature [MAT]) and dry climate (<1 m annual rainfall). Dry conditions are also indicated by the abundance of fresh plagioclase, smectite clay, and gypsum pseudomorphs in the paleosols. However, features of *Javelinoxylon* wood anatomy indicate almost complete lack of seasonality in temperature or water availability. Warm and dry, but nonseasonal, climates are uncommon today. For example, constraints based on paleosol isotope data and fossil wood anatomy suggest that Javelina climatic conditions were comparable to modern tropical or subtropical steppe (modified Köppen global climate classification; Trewartha, 1968). These climatic regions typically have a pronounced summer or winter dry season, with grassland or woodland vegetation, and true forest is rare. In contrast, during deposition of the Javelina Formation, similar low annual rainfall was apparently distributed more uniformly over the year and resulted in a closed canopy forest. This nonseasonal subtropical steppe climate may have been preferred by azhdarchid pterosaurs.

If the assemblage of *Quetzalcoatlus lawsoni* preserved at the Amaral Site represents a migratory flock, it seems most likely that their movement had been to or from feeding or nesting areas. Because the Late Cretaceous latitudinal temperature gradient was so low, and the subtropical climatic zone lacked seasonality, if pterosaur populations underwent migration, it was probably not in response to strong seasonality, as is typically the case with many migratory birds today.

## SUMMARY AND HABITAT RECONSTRUCTION

One of the aims of paleontology and sedimentology is to provide an accurate reconstruction of past environments, and to place extinct organisms in their former habitats. Such reconstructions should be based, as much as possible, on well-documented observations and comparison with modern examples, rather than guesswork. Of course, any reconstruction only reflects the present understanding and so will be continually modified as new information comes to light. Moreover, given the few specimens thus far known, suggestions regarding the lifestyle of *Quetzalcoatlus* offered here must remain speculative. Figure 18 and what follows is a reconstruction of the habitat of *Quetzalcoatlus* resulting from the present study.

For the purposes of the following reconstruction, it is informative to delineate present-day areas that have climatic conditions similar to those postulated for the dry subtropical environment of *Quetzalcoatlus*. Evidence from paleosols, flora, and isotope geochemistry indicate that this environment was characterized by (1) a mean annual temperature ca. 20°C, (2) annual rainfall generally less than 1 m, and (3) a lack of pronounced seasonality (for comparison, an annual range of mean monthly temperatures of less than 5°C and rainfall distributed over more than 100 days per year are assumed). In North America today, these conditions are met only in parts of southern Mexico (the coastal plains of Oaxaca, Chiapas, and Yucatan; Shelford, 1963). In this area, the dry interior mountainous regions support grassland, savanna, or a mixed conifer and oak forest. The wet inland regions support a luxuriant evergreen tropical rainforest. However, the drier coastal plains support a deciduous or semideciduous tropical forest, including present-day representatives of malvalean trees (e.g., *Ceiba*, *Sterculia*), palms, and crocodilians, under conditions similar to those postulated for the Javelina depositional environment.

The Late Cretaceous Tornillo Basin was a broad alluvial valley, ca. 50–100 km across, flanked by low hills that exposed older Cretaceous strata. The surrounding terrain had little topographic relief, there were no nearby mountain ranges, and the climate was warm, dry, and nonseasonal. Flowing along the axis of the valley was the main trunk stream of a meandering river system that drained volcanic terrain northwest of the basin and continued to its mouth along the shoreline in northern Mexico several hundred kilometers to the southeast. The river channel was 40–50 m wide, with flow fluctuating dramatically. During flood events, water in the channel was 3–4 m deep, whereas during periods of reduced flow the current was diverted around emergent sand bars and fallen logs. An aquatic fauna of gar and amiid fishes, turtles, and crocodilians inhabited the active stream channel.

Alluvial soils on the floodplain surrounding the river supported a mixed semideciduous or evergreen forest dominated by the dicot *Javelinoxylon* with araucariacean conifers as isolated emergents. Mature stands of forest had a canopy height over 30 m. The floodplain forest sustained a fauna dominated by the sauropod dinosaur *Alamosaurus*. This large herbivore was capable of browsing to a height of 8–10 m above the forest floor and so may have avoided the high mature forest, instead feeding where the canopy was lower along stream courses and in areas of regrowth around windfalls.

Standing water in abandoned reaches of the stream channel formed shallow alkaline lakes. Continued inflow of river water was balanced by outflow, so that the lakes did not become saline through evaporation. Palms and aquatic vines grew around the shoreline. Sediment accumulated in the lakes episodically, when nearby active stream channels were flooding,

Downloaded From: https://bioone.org/journals/Journal-of-Vertebrate-Paleontology on 24 Apr 2024
Terms of Use: https://bioone.org/terms-of-use

FIGURE 18. Reconstruction of *Quetzalcoatlus lawsoni*, sp. nov., in abandoned channel-lake habitat. Areas bordering lake are vegetated with fan palms, and distant floodplain forest supports an evergreen tropical forest composed predominantly of the dicot tree *Javelinoxylon multiporosum* with isolated emergent araucariacean conifers. A flock of pterosaurs is shown landing, standing, and feeding in various suggested postures.

and during intervening periods carbonate sediment precipitated from the water, owing to algal and microbial activities. At times, a diverse invertebrate fauna of crustaceans, worms, snails, and clams inhabited the lake bottoms. Flocks of the pterosaur *Quetzalcoatlus lawsoni* frequented the areas around the lakes, feeding in shallow water, using their long beaks to probe for burrowing lacustrine invertebrates, and may have nested on the ground among the palms surrounding the lakes. *Quetzalcoatlus northropi* appears instead to have favored riparian environments and may have led a more solitary lifestyle.

## ACKNOWLEDGMENTS

W. Langston, Jr., dedicated over 30 years of painstaking effort to collecting, preparing, restoring, reconstructing, and studying the pterosaur specimens recovered in Big Bend National Park (Bell et al., 2013). The research described herein began in 1993 as a collaborative effort between the author and Langston to document the stratigraphic and paleoenvironmental contexts of the pterosaur-bearing localities and to provide background for Langston's osteological work on the specimens. Although a preliminary account of the present research was given at the annual meeting of the Society of Vertebrate Paleontology in 1996 (Lehman and Langston, 1996), work continued in collaboration intermittently over the ensuing 17 years but was not completed to Langston's satisfaction at the time of his death in 2013. It should be clear that the present study would not have been possible without Langston's support and guidance, initially as a teacher and mentor, and later as a colleague. In particular, the section regarding taphonomy is based largely on Langston's observations. He inculcated in his students an appreciation for the sedimentary context of vertebrate fossils, and the present study was an attempt to follow his instruction. The Science and Resource Management personnel of Big Bend National Park, in particular S. Wick, P. Koepp, M. Fleming, and D. Corrick, have assisted the author for many years in conducting field work in the park. Specimens discussed in this study were collected under the authority of successive Antiquities Act permits granted to Wann Langston, Jr., from 1973 to 1991. H. Karlsson, J. Browning, V. Upton, and K. Ferguson performed the isotopic analyses reported herein and assisted with interpretation. M. Gower and J. Browning prepared the thin sections used in this study. S. Wick, S. Tomlinson, and W. Straight assisted the author with field work. K. Padian, B. Andres, and two anonymous reviewers provided helpful comments on the manuscript, and the Department of Geosciences at Texas Tech University provided assistance for its preparation. All drawings and illustrations are the work of the author.

Downloaded From: https://bioone.org/journals/Journal-of-Vertebrate-Paleontology on 24 Apr 2024
Terms of Use: https://bioone.org/terms-of-use

## LITERATURE CITED


Anadon, P., and R. Utrilla. 1993. Sedimentology and isotope geochemistry of lacustrine carbonates of the Oligocene Campins Basin, northeast Spain. Sedimentology 40:699–720.

Andres, B. and Langston W. 2021. Morphology and taxonomy of *Quetzalcoatlus* (Pterodactyloidea: Azhdarchoidea); pp. 46–202 in K. Padian and M.A. Brown (eds.), The Late Cretaceous pterosaur *Quetzalcoatlus* Lawson 1975 (Pterodactyloidea: Azhdarchoidea). Society of Vertebrate Paleontology Memoir 19. Journal of Vertebrate Paleontology 41(2, Supplement).

Arambourg, C. 1959. *Titanopteryx philadelphiae* nov. gen., nov. sp., ptérosaurien géant. Notes et Mémoires sur le Moyen-Orient 7:229–234.

Archibald, J. D., and H. D. Sues. 1998. Precis of the Cretaceous paleontology, biostratigraphy, and sedimentology at Dzharakuduk (Turonian?-Santonian), Kyzylkum Desert, Uzbekistan. New Mexico Museum of Natural History and Science Bulletin 14:21–28.

Atchley, S. C., L. C. Nordt, and S. J. Dworkin. 2004. Eustatic control on alluvial sequence stratigraphy: a possible example from the Cretaceous-Tertiary transition of the Tornillo Basin, Big Bend National Park, West Texas, U.S.A. Journal of Sedimentary Research 74:391–404.

Averianov, A. O. 2007. New records of azhdarchids (Pterosauria, Azhdarchidae) from the Late Cretaceous of Russia, Kazakhstan, and Central Asia. Paleontological Journal 41:189–197.

Badgley, C. 1986. Counting individuals in mammalian fossil assemblages from fluvial environments. Palaios 1:328–338.

Bakhurina, N. N., and D. M. Unwin. 1995. A survey of pterosaurs from the Jurassic and Cretaceous of the former Soviet Union and Mongolia. Historical Biology 10:197–245.

Behrensmeyer, A. K. 1978. Taphonomic and ecologic information from bone weathering. Paleobiology 4:150–162.

Behrensmeyer, A. K. 1991. Terrestrial vertebrate accumulations; pp. 291–335 in P. A. Allison and D. E. Briggs (eds.), Taphonomy: Releasing the Data Locked in the Fossil Record. Plenum Press, New York.

Bell, C. J., M. A. Brown, M. R. Dawson, and E. L. Lundelius. 2013. Wann Langston, Jr.—a life amongst bones. Earth and Environmental Science Transactions of the Royal Society of Edinburgh 103:189–204.

Bell, C. M., and K. Padian. 1995. Pterosaur fossils from the Cretaceous of Chile: evidence for a pterosaur colony on an inland desert plain. Geological Magazine 132:31–38.

Beurden, K. 1971. As condicoes ecologicas e faciologicas da Formacao Santana na Chapada do Araripe (Nordeste do Brasil). Anais da *Academia* Brasileira de Ciências (Suplemento) 43:411–415.

Bickart, K. J. 1984. A field experiment in avian taphonomy. Journal of Vertebrate Paleontology 4:525–535.

Blakey, R. C., and W. D. Ranney. 2018. Ancient Landscapes of Western North America: A Geologic History with Paleogeographic Maps. Springer Nature, Cham, Switzerland, 228 pp.

Bown, T. M., and M. J. Kraus. 1981. Lower Eocene alluvial paleosols (Willwood Formation, northwest Wyoming, U.S.A.) and their significance for paleoecology, paleoclimatology, and basin analysis. Palaeogeography, Palaeoclimatology, Palaeoecology 34:1–30.

Bown, T. M., and M. J. Kraus. 1983. Ichnofossils of the alluvial Willwood Formation (Lower Eocene), Bighorn Basin, Northwest Wyoming, U.S.A. Palaeogeography, Palaeoclimatology, Palaeoecology 43:95–128.

Brown, M. A., J. C. Sagebiel, and B. Andres. 2021. The discovery, local distribution, and curation of the giant azhdarchid pterosaurs from Big Bend National Park; pp. 2–20 in K. Padian and M.A. Brown (eds.), The Late Cretaceous pterosaur *Quetzalcoatlus* Lawson 1975 (Pterodactyloidea: Azhdarchoidea). Society of Vertebrate Paleontology Memoir 19. Journal of Vertebrate Paleontology 41(2, Supplement).

Buffetaut, E. 1995. The importance of 'Lagerstätten' for our understanding of the evolutionary history of certain groups of organisms: the case for the pterosaurs; pp. 49–52 in M.N. Melendez (ed.) in II International Symposium on Lithographic Limestones, Ediciones de la Universidad Autónoma de Madrid, Lleida-Cuenca, Spain.

Buffetaut, E., D. Grigorescu, and Z. Csiki. 2002. A new giant pterosaur with a robust skull from the latest Cretaceous of Romania. Naturwissenschaften 89:180–184.

Buffetaut, E., D. Grigorescu, and Z. Csiki. 2003. Giant azhdarchid pterosaurs from the terminal Cretaceous of Transylvania (western Romania). Geological Society of London, Special Publications 217:91–104.

Cai, Z., and F. Wei. 1994. *Zhejiangopterus linhaiensis* (Pterosauria) from the Upper Cretaceous of Linhai, Zhejiang, China. Vertebrata Palasiatica 32:181–194.

Carpenter, K. 1990. Variation in *Tyrannosaurus rex*; pp. 141–145 in K. Carpenter and P. J. Currie (eds.), Dinosaur Systematics: Perspectives and Approaches. Cambridge University Press, Cambridge, U.K.

Cerling, T. E. 1984. The stable isotopic composition of soil carbonate and its relationship to climate. Earth and Planetary Science Letters 71:229–240.

Cerling, T. E., and R. L. Hay. 1986. An isotopic study of paleosol carbonates from Olduvai Gorge. Quaternary Research 25:63–78.

Cerling, T. E., J. R. Bowman, and J. R. O'Neil. 1988. An isotopic study of a fluvial-lacustrine sequence: the Plio-Pleistocene Koobi Fora sequence, East Africa. Palaeogeography, Palaeoclimatology, Palaeoecology 63:335–356.

Chatterjee, S., and R. J. Templin. 2004. Posture, locomotion, and paleoecology of pterosaurs. Geological Society of America, Special Paper 376:1–64.

Company, J., J. Ruiz-Omenaca, and X. Pereda-Suberbiola. 1999. A long-necked pterosaur (Pterodactyloidea, Azhdarchidae) from the Upper Cretaceous of Valencia, Spain. Geologie en Mijnbouw 78:319–333.

Dworkin, S. L., L. Nordt, and S. Atchley. 2005. Determining terrestrial paleotemperatures using the oxygen isotopic composition of pedogenic carbonate. Earth and Planetary Science Letters 237:56–68.

Estes, R. 1964. Fossil vertebrates from the Late Cretaceous Lance Formation, eastern Wyoming. University of California Publications in Geological Science 49:1–180.

Ethridge, F. G., and S. A. Schumm. 1978. Reconstructing paleochannel morphologic and flow characteristics: methodology, limitations, and assessment; pp. 703–721 in A. D. Miall (ed.), Fluvial Sedimentology, Canadian Society of Petroleum Geologists Memoir 5. Alberta, Canada.

Ferguson, K. M., T. M. Lehman, and R. T. Gregory. 1991. C- and O-isotopes of pedogenic soil nodules from two sections spanning the K-T transition in West Texas. Geological Society of America, Abstracts with Programs 23:302.

Frey, E., and D. M. Martill. 1994. A new pterosaur from the Crato Formation (Lower Cretaceous, Aptian) of Brazil. Neues Jahrbuch für Geologie und Paläontologie, Abhandlungen 194:379–412.

Frey, E., and D. M. Martill. 1996. A reappraisal of *Arambourgania* (Pterosauria, Pterodactyloidea): one of the world's largest flying animals. Neues Jahrbuch für Geologie und Paläontologie, Abhandlungen 199:221–247.

Fronimos, J. A., and T. M. Lehman. 2014. New specimens of a titanosaur sauropod from the Maastrichtian of Big Bend National Park, Texas. Journal of Vertebrate Paleontology 34:883–899.

Fry, B., and E. B. Sherr. 1984. $\delta^{13}C$ measurements as indicators of carbon flow in marine and freshwater ecosystems. Contributions in Marine Science 27:13–47.

Gerdes, G., K. Dunajtschik, H. Riege, A. G. Taher, W. E. Krumbein, and H. E. Reineck. 1994. Structural diversity of biogenic carbonate particles in microbial mats. Sedimentology 41:1273–1294.

Gilinsky, N. L., and J. B. Bennington. 1994. Estimating numbers of whole individuals from collections of body parts: a taphonomic limitation of the paleontological record. Paleobiology 20:245–258.

Godfrey, S. J., and P. J. Currie. 2005. Pterosaurs; pp. 292–311 in P. J. Currie and E. B. Koppelhus (eds.), Dinosaur Provincial Park: A Spectacular Ancient Ecosystem Revealed. Indiana University Press, Bloomington, Indiana.

Gregory, R. T., C. B. Douthitt, I. R. Duddy, P. V. Rich, and T. H. Rich. 1989. Oxygen isotope composition of carbonate concretions from the Lower Cretaceous of Victoria, Australia: implications for the evolution of meteoric waters on the Australian continent in a paleopolar environment. Earth and Planetary Science Letters 92:27–42.

Henderson, M. D., and J. E. Peterson. 2006. An azhdarchid pterosaur cervical vertebra from the Hell Creek Formation (Maastrichtian) of southeastern Montana. Journal of Vertebrate Paleontology 26:192–195.

Hill, A. P. 1980. Early post mortem damage to the remains of some contemporaneous East African mammals; pp. 131–152 in A. K.


Downloaded From: https://bioone.org/journals/Journal-of-Vertebrate-Paleontology on 24 Apr 2024
Terms of Use: https://bioone.org/terms-of-use

Behrensmeyer and A. P. Hill (eds.), Fossils in the Making. University of Chicago Press, Chicago, Illinois.
Hill, A. P., and A. Walker. 1972. Procedures in vertebrate taphonomy; notes on a Uganda Miocene fossil locality. Journal of the Geological Society of London 128:399–406.
Hunt, R. K., and T. M. Lehman. 2008. Attributes of the ceratopsian dinosaur *Torosaurus*, and new material from the Javelina Formation (Maastrichtian) of Texas. Journal of Paleontology 82:1127–1138.
Johnsgard, P. A. 1983. Cranes of the World. Indiana University Press, Bloomington, Indiana, 257 pp.
Johnson, E. 1985. Current developments in bone technology; pp. 157–235 in M. B. Schiffer (ed.), Advances in Archaeological Method and Theory, Volume 8. Academic Press, New York.
Kellner, A. 1994. Remarks on pterosaur taphonomy and paleoecology. Acta Geologica Leopoldensia 17:175–189.
Kellner, A., and W. L. Langston Jr. 1996. Cranial remains of *Quetzalcoatlus* (Pterosauria, Azhdarchidae) from Late Cretaceous sediments of Big Bend National Park, Texas. Journal of Vertebrate Paleontology 16:222–231.
Kelts, K., and K. J. Hsu. 1978. Freshwater carbonate sedimentation; pp. 295–323 in A. Lerman (ed.), Lakes, Chemistry, Geology, and Physics. Springer, New York.
Klein, R. G., and K. Cruz-Uribe. 1984. The Analysis of Animal Bones from Archeological Sites. University of Chicago Press, Chicago, Illinois, 273 pp.
Langston, W., Jr. 1978. The great pterosaur. Discovery, University of Texas at Austin 2:20–23.
Langston, W., Jr. 1981. Pterosaurs. Scientific American 244:122–136.
Langston, W., Jr., B. Standhardt, and M. Stevens. 1989. Fossil vertebrate collecting in the Big Bend—history and retrospective; pp. 11–21 in A. B. Busbey and T. M. Lehman (eds.), Vertebrate Paleontology, Biostratigraphy, and Depositional Environments, Latest Cretaceous and Tertiary, Big Bend Area, Texas. 49th Annual Meeting of the Society of Vertebrate Paleontology, Field Trip Guidebook. Deerfield, Illinois.
Lawson, D. A. 1972. Paleoecology of the Tornillo Formation, Big Bend National Park, Brewster County, Texas. M.A. thesis, University of Texas, Austin, Texas, 182 pp.
Lawson, D. A. 1975a. Pterosaur from the latest Cretaceous of west Texas, discovery of the largest flying creature. Science 187:947–948.
Lawson, D. A. 1975b. Could pterosaurs fly? [Response to Greenewalt]. Science 188:676–677.
Lawson, D. A. 1976. *Tyrannosaurus* and *Torosaurus*, Maastrichtian dinosaurs from Trans-Pecos Texas. Journal of Paleontology 50:158–164.
Lehman, T. M. 1987. Late Maastrichtian paleoenvironments and dinosaur biogeography in the western interior of North America. Palaeogeography, Palaeoclimatology, Palaeoecology 60:189–217.
Lehman, T. M. 1988. Stratigraphy of the Cretaceous-Tertiary and Paleocene-Eocene transition rocks of Big Bend, a discussion. Journal of Geology 96:627–631.
Lehman, T. M. 1989. Upper Cretaceous (Maastrichtian) paleosols in Trans-Pecos Texas. Geological Society of America Bulletin 101:188–203.
Lehman, T. M. 1990. Paleosols and the Cretaceous/Tertiary transition in the Big Bend region of Texas. Geology 18:362–364.
Lehman, T. M. 1991. Sedimentation and tectonism in the Laramide Tornillo Basin of West Texas. Sedimentary Geology 75:9–28.
Lehman, T. M. 1996. A horned dinosaur from the El Picacho Formation of west Texas, and review of ceratopsian dinosaurs from the American Southwest. Journal of Paleontology 70:494–508.
Lehman, T. M. 2002. Revisions to the Tornillo Group (Upper Cretaceous–Eocene), Big Bend National Park, Texas. Geological Society of America, Abstracts with Programs 34:A–10.
Lehman, T. M. 2007. Upper Cretaceous and Paleogene strata south of the Chisos Mountains, Big Bend National Park, Texas. Geological Society of America, Abstracts with Programs 39:510.
Lehman, T. M., and K. Barnes. 2010. *Champsosaurus* (Diapsida: Choristodera) from the Paleocene of West Texas: paleoclimatic implications. Journal of Paleontology 84:341–345.
Lehman, T. M., and A. Busbey. 2007. Big Bend Field Trip Field Guide. Society of Vertebrate Paleontology, 2007 Annual Meeting Field Trip. Deerfield, Illinois, 69 pp.
Lehman, T. M., and A. B. Coulson. 2002. A juvenile specimen of the sauropod dinosaur *Alamosaurus sanjuanensis* from the Upper Cretaceous of Big Bend National Park, Texas. Journal of Paleontology 76:156–172.
Lehman, T. M., and W. Langston Jr. 1996. Habitat and behavior of *Quetzalcoatlus*: paleoenvironmental reconstruction of the Javelina Formation (Upper Cretaceous), Big Bend National Park, Texas. Journal of Vertebrate Paleontology 16(3, Supplement):48A.
Lehman, T. M., F. W. McDowell, and J. N. Connelly. 2006. First isotopic (U-Pb) age for the Late Cretaceous *Alamosaurus* vertebrate fauna of West Texas, and its significance as a link between two faunal provinces. Journal of Vertebrate Paleontology 26:922–928.
Lehman, T. M., S. L. Wick, and J. R. Wagner. 2016. Hadrosaurian dinosaurs from the Maastrichtian Javelina Formation, Big Bend National Park, Texas. Journal of Paleontology 90:333–356.
Leslie, C. E., D. J. Peppe, T. E. Williamson, M. Heizler, M. Jackson, S. C. Atchley, L. Nordt, and B. Standhardt. 2018. Revised age constraints for Late Cretaceous to early Paleocene terrestrial strata from the Dawson Creek section, Big Bend National Park, West Texas. Geological Society of America Bulletin. doi: 10.1130/B31785.1.
Lewy, Z., A. C. Milner, and C. Patterson. 1992. Remarkably preserved natural endocranial casts of pterosaurs and fish from the Late Cretaceous of Israel. Geological Survey of Israel Current Research 7:31–35.
Lyman, R. L. 1994. Vertebrate Taphonomy. Cambridge University Press, Cambridge, U.K., 524 pp.
Mack, G. H., W. C. James, and H. C. Monger. 1993. Classification of paleosols. Geological Society of America Bulletin 105:129–136.
Manchester, S. R., T. M. Lehman, and E. A. Wheeler. 2010. Fossil palms (Arecaceae, Coryphoideae) associated with juvenile herbivorous dinosaurs in the Upper Cretaceous Aguja Formation, Big Bend National Park, Texas. International Journal of Plant Sciences 171:679–689.
Martin, R. E. 1999. Taphonomy, A Process Approach. Cambridge University Press, Cambridge, U.K., 508 pp.
McGowen, M. R., K. Padian, M. A. de Sosa, and R. J. Harmon. 2002. Description of *Montanazhdarcho minor*, an azhdarchid pterosaur from the Two Medicine Formation (Campanian) of Montana. PaleoBios 22:1–9.
Miall, A. D. 1978. Lithofacies types and vertical profile models in braided river deposits, a summary; pp. 597–604 in A. D. Miall (ed.), Fluvial Sedimentology. Canadian Society of Petroleum Geology Memoir 5. Alberta, Canada.
Nesov, L. A. 1984. Upper Cretaceous pterosaurs and birds from central Asia. Paleontological Journal 18:38–49.
Nesov, L. A. 1991a. [Flying reptiles over sycamore-tree forests and brackish sea bays]. Herpetological Researches—Paleontology (Leningrad) 1:147–163. [Russian]
Nesov, L. A. 1991b. [Giant flying reptiles of the Family Azhdarchidae], Morfologiya, Sistematika. Bulletin of the University of Leningrad 1991, Series 7, Geology/Geography 2(14):4–23. [Russian]
Nesov, L. A. 1991c. [Giant flying reptiles of the Family Azhdarchidae II. Habitat, Sedimentology, and Taphonomy of Burial Circumstances]. Bulletin of the University of Leningrad 1991, Series 7, Geology/Geography 3(21):15–24. [Russian]
Nordt, L., S. Atchley, and S. Dworkin. 2003. Terrestrial evidence for two greenhouse events in the latest Cretaceous. GSA Today 14(12):4–9.
Osmond, C. B., N. Valaane, S. M. Haslam, P. Uotila, and Z. Roksandic. 1981. Comparisons of δ13C values in leaves of aquatic macrophytes from different habitats in Britain and Finland, some implications for photosynthetic processes in aquatic plants. Oecologia 50:117–124.
Padian, K., and M. Smith. 1992. New light on Late Cretaceous pterosaur material from Montana. Journal of Vertebrate Paleontology 12:87–92.
Retallack, G. J. 1983. Late Eocene and Oligocene Paleosols from Badlands National Park, South Dakota. Geological Society of America Special Paper 193. Boulder, Colorado, 82 pp.
Rohr, D. M., A. J. Boucot, J. Miller, and M. Abbott. 1986. Oldest termite nest from the Upper Cretaceous of West Texas. Geology 14:87–88.
Schäfer, W. 1962. Aktuo-Paläeontologie nach Studien in der Nordsee. Verlag Waldemar Kramer, Frankfort, Germany, 166 pp.
Schmidt, D. R. 2009. Stable isotope geochemistry of Upper Cretaceous and Paleocene strata in Big Bend National Park, Texas. Ph.D. thesis, Texas Tech University, Lubbock, Texas, 202 pp.
Schumm, S. A. 1960. The Shape of Alluvial Channels in Relation to Sediment Type. U.S. Geological Survey Professional Paper 352-B. Reston, Virginia, 30 pp.
Seilacher, A. 1970. Begriff und Bedeutung der Fossil-Lagerstatten. Neues Jahrbuch für Geologie und Paläontologie, Monatshafte 1970:34–39.

Downloaded From: https://bioone.org/journals/Journal-of-Vertebrate-Paleontology on 24 Apr 2024
Terms of Use: https://bioone.org/terms-of-use

Shelford, V. E. 1963. The Ecology of North America. University of Illinois Press, Urbana, Illinois, 610 pp.
Shipman, P. 1981. Life History of a Fossil: An Introduction to Taphonomy and Paleoecology. Harvard University Press, Cambridge, Massachusetts, 222 pp.
Smith, N. D., and M. Pérez-Arlucea. 1994. Fine-grained deposition in the avulsion belt of the Lower Saskatchewan River, Canada. Journal of Sedimentary Research B64:159–168.
Smith, R. M. H. 1987. Morphology and depositional history of exhumed Permian point bars in the southwestern Karoo, South Africa. Journal of Sedimentary Petrology 57:19–29.
Sneh, A. 1983. Desert stream sequences in the Sinai Peninsula. Journal of Sedimentary Petrology 53:1271–1279.
Standhardt, B. R. 1986. Vertebrate paleontology of the Cretaceous/Tertiary transition of Big Bend National Park, Texas. Ph.D. dissertation, Louisiana State University, Baton Rouge, Louisiana, 298 pp.
Stear, W. M. 1983. Morphological characteristics of ephemeral stream channel and overbank splay sandstone bodies in the Permian Beaufort Group, Karoo Basin, South Africa; pp. 405–420 in J. D. Collinson and J. Lewin (eds.), Modern and Ancient Fluvial Systems. International Association of Sedimentologists Special Publication 6. London, U.K.
Suberbiola, X. P., N. Bardet, S. Jouve, M. Iarochène, B. Bouya, and M. Amaghzaz. 2003. A new azdarchid pterosaur from the Late Cretaceous phosphates of Morocco. Geological Society, London, Special Publications 217:79–90.
Talbot, M. R., and K. Kelts. 1990. Paleolimnological signatures from carbon and oxygen isotopic ratios in carbonates from organic carbon-rich lacustrine sediments; pp. 99–112 in B. J. Katz (ed.), Lacustrine Basin Exploration. American Association of Petroleum Geologists Memoir 50. Tulsa, Oklahoma.
Trewartha, G. T. 1968. An Introduction to Climate. McGraw-Hill, New York, 408 pp.
Tunbridge, I. P. 1984. Facies model for a sandy ephemeral stream and clay playa complex: the Middle Devonian Trentishoe Formation of North Devon, U.K. Sedimentology 31:697–715.
Tykoski, R. S., and A. R. Fiorillo. 2016. An articulated series of *Alamosaurus sanjuanensis* Gilmore, 1922 (Dinosauria, Sauropoda) from Texas: new perspective on the relationships of North America's last giant sauropod. Journal of Systematic Palaeontology 15:339–364.
Unwin, D. M., and N. N. Bakhurina. 2000. Pterosaurs from Russia, middle Asia, and Mongolia; pp. 420–433 in M. J. Benton, M. A. Shishkin, D. M. Unwin, and E. N. Kurochkin (eds.), The Age of Dinosaurs in Russia and Mongolia. Cambridge University Press, Cambridge, U.K.
Voorhies, M. R. 1969. Taphonomy and Population Dynamics of an Early Pliocene Vertebrate Fauna, Knox County, Nebraska. University of Wyoming Contributions to Geology, Special Paper 1. Laramie, Wyoming, 69 pp.
Vremir, M., A. W. Kellner, D. Naish, and G. J. Dyke. 2013. A new azhdarchid pterosaur from the Late Cretaceous of the Transylvanian Basin, Romania: implications for azhdarchid diversity and distribution. PLoS ONE 8:e54268. doi: 10.1371/journal.pone.0054268.
Weigelt, J. 1989. Recent Vertebrate Carcasses and Their Paleontological Implications (translated by Judith Schaefer). University of Chicago Press, Chicago, Illinois, 188 pp.
Wellnhofer, P. 1970. Die Pterodactyloidea (Pterosauria) der Oberjura-Plattenkalke Südeutschlands. Abhandlungen der Bayerische Akademie der Wissenschaften Mathematisch Naturwissenschaftliche Klasse, Neue Folge 141:1–133.
Wellnhofer, P. 1991. The Illustrated Encyclopedia of Pterosaurs. Crescent Books, New York, 192 pp.
Wells, N. A. 1983. Transient streams in sand-poor redbeds: Early-Middle Eocene Kuldana Formation of northern Pakistan; pp. 393–403 in J. D. Collinson and J. Lewin (eds.), Modern and Ancient Fluvial Systems. International Association of Sedimentologists Special Publication 6. London, U.K.
Wheeler, E. A., and T. M. Lehman. 2000. Late Cretaceous woody dicots from the Aguja and Javelina formations, Big Bend National Park, Texas, USA. International Association of Wood Anatomists Journal 21:83–120.
Wheeler, E. A., and T. M. Lehman. 2005. Upper Cretaceous–Paleocene conifer woods from Big Bend National Park, Texas, USA. Palaeogeography, Palaeoclimatology, Palaeoecology 226:233–258.
Wheeler, E. A., T. M. Lehman, and P. Gasson. 1994. *Javelinoxylon*, a new genus of malvalean tree from the Upper Cretaceous of Big Bend National Park, Texas. American Journal of Botany 81:703–710.
Wick, S. L. 2014. New evidence for the possible occurrence of *Tyrannosaurus* in West Texas, and discussion of Maastrichtian tyrannosaurid dinosaurs from Big Bend National Park. Cretaceous Research 50:52–58.
Wick, S. L., and T. M. Lehman. 2013. A new ceratopsian dinosaur from the Javelina Formation (Maastrichtian) of West Texas and implications for chasmosaurine phylogeny. Naturwissenschaften 100:667–682.
Witton, M. P., and M. B. Habib. 2010. On the size and flight diversity of giant pterosaurs, the use of birds as pterosaur analogues and comments on pterosaur flightlessness. PLoS ONE 5:e13982. doi: 10.1371/journal.pone.0013982.

Submitted October 11, 2017; revisions received July 9, 2018;
accepted September 13, 2018.
Memoir Editor: Randall Irmis.

Downloaded From: https://bioone.org/journals/Journal-of-Vertebrate-Paleontology on 24 Apr 2024
Terms of Use: https://bioone.org/terms-of-use